PHYSICAL REVIEW C **72**, 044001 (2005)

Isospin-violating nucleon-nucleon forces using the method of unitary transformation

E. Epelbaum[1,*] and Ulf-G. Meißner[2,3,†]
[1]*Jefferson Laboratory, Theory Division, Newport News, Virginia 23606, USA*
[2]*Universität Bonn, Helmholtz-Institut für Strahlen- und Kernphysik (Theorie), D-53115 Bonn, Germany*
[3]*Forschungszentrum Jülich, Institut für Kernphysik (Theorie), D-52425 Jülich, Germany*
(Received 25 February 2005; published 3 October 2005)

Recently, we have derived the leading and subleading isospin-breaking three-nucleon forces using the method of unitary transformation. In the present work we extend this analysis and consider the corresponding two-nucleon forces using the same approach. Certain contributions to the isospin-violating one- and two-pion-exchange potential have already been discussed by various groups within the effective field theory framework. Our findings agree with the previously obtained results. In addition, we present the expressions for the subleading charge-symmetry-breaking two-pion exchange potential which were not considered before. These corrections turn out to be numerically important. Together with the three-nucleon force results presented in our previous work, the results of the present study specify completely isospin-violating nuclear forces up to the order q^5/Λ^5, where q (Λ) denotes the soft (hard) scale.

DOI: 10.1103/PhysRevC.72.044001 PACS number(s): 21.45.+v, 21.30.−x, 25.10.+s

I. INTRODUCTION

The interactions between two nucleons are one of the best studied strong interaction processes, which is due to the large database of proton-proton and neutron-proton scattering experiments. As such, many fine features of the strong interactions and their interplay with the electromagnetic and weak interactions can be unraveled from such studies, provided a sufficiently accurate theoretical tool is available to match the sometimes astonishing precision of the data. In this paper, we are interested in the effects of isospin violation in the two-nucleon sector. Although isospin is an approximate symmetry of the QCD Lagrangian, the difference in the up and down quark masses combined with the long-range electromagnetic force leads to appreciable deviations from the isospin limit. To quantify these effects, it is mandatory to have a framework that consistently incorporates these various sources. Such a scheme has been developed in the last decade, namely chiral nuclear effective field theory. It extends the so successful chiral perturbation theory for mesons and meson-baryon systems to processes involving $2, 3, 4, \ldots$ nucleons. Chiral nuclear effective field theory, (EFT) has already been applied to study isospin-violating two-nucleon forces (2NFs), see, e.g., Refs. [1–8]. So why come back to this topic? Recently, we have derived the leading and subleading isospin-breaking three-nucleon forces (3NFs) using the method of unitary transformation [9]. In the present work, we will apply this framework to study the corresponding isospin-breaking two-nucleon forces at the same order in the low-momentum expansion. Thereby, we will rederive the many interesting results already obtained in the earlier studies, but also work out the contributions, which have were never been studied before. To the order we are working, we have thus constructed the complete set of isospin-violating few-nucleon forces.

The material in this paper is organized as follows. In Sec. II we discuss the effective Lagrangian underlying our calculation and also the corresponding power counting. Section III is devoted to the derivation of the isospin-violating 2NFs, consisting of the one- and two-pion-exchange potentials and the corresponding contact interactions. The main novelty is the next-to-leading order two-pion-exchange potential, which is derived here in its complete form for the first time and also turns out to be numerically large, very similar to the isospin-conserving case. In Sec. IV we demonstrate explicitly the consistency between the two-nucleon forces derived here and the corresponding isospin-violating three-nucleon forces obtained in Ref. [9]. Section V contains the summary and outlook.

II. POWER COUNTING AND EFFECTIVE LAGRANGIAN

Within the Standard Model, isospin violation has its origin in the different masses of the up and down quarks and the electromagnetic interactions. At low energy, isospin-breaking effects in few-nucleon systems can be studied in the systematic and model-independent framework of chiral effective field theory. This method is based on the most general (approximatively) chiral invariant Lagrangian for pions and nucleons which includes all possible interactions consistent with the isospin violation in the underlying theory. Consider first isospin breaking in the strong interactions. The QCD quark mass term can be expressed in the two-flavor case as

$$\mathcal{L}_{\rm mass}^{\rm QCD} = -\tfrac{1}{2}\bar{q}(m_u + m_d)(1 + \epsilon\tau_3)\,q,$$

where

$$\epsilon \equiv \frac{m_u - m_d}{m_u + m_d} \sim -\frac{1}{3}. \qquad (2.1)$$

The above numerical estimation is based on the light quark mass values utilizing a modified $\overline{\rm MS}$ subtraction scheme at a renormalization scale of 1 GeV [10]. The isoscalar term in

*Electronic address: epelbaum@jlab.org
†Electronic address: meissner@itkp.uni-bonn.de; URL: www.itkp.uni-bonn.de/ meissner/

Eq. (2.1) breaks chiral but preserves isospin symmetry. It leads to the nonvanishing pion mass, $M^2 = (m_u + m_d)B \neq 0$, where B is a low-energy constant (LEC) that describes the strength of the bilinear light quark condensate. Further, this term generates a string of chiral-symmetry-breaking interactions in the effective Lagrangian which are proportional to positive powers of M^2. The isovector term ($\propto \tau_3$) in Eq. (2.1) breaks isospin symmetry and generates a series of isospin-breaking effective interactions $\propto (\epsilon M^2)^n$ with $n \geqslant 1$. It is, therefore, natural to count strong isospin violation in terms of ϵM^2.[1]

Electromagnetic terms in the effective Lagrangian can be generated using the method of external sources, see, e.g., Refs. [1,11–13] for more details. All such terms are proportional to the nucleon charge matrix $Q = e(1 + \tau_3)/2$, where e denotes the electric charge.[2] More precisely, the vertices which contain (do not contain) the photon fields are proportional to Q^n (Q^{2n}), where $n = 1, 2, \ldots$. Since we are interested here in nucleon-nucleon scattering in the absence of external fields, so that no photon can leave a Feynman diagram, it is convenient to introduce the small parameter $e^2 \sim 1/10$ for isospin-violating effects caused by the electromagnetic interactions.

In the present study we adopt the same power counting rules for isospin-breaking contributions as specified in Ref. [9]. In particular, we count

$$\epsilon \sim e \sim \frac{q}{\Lambda}; \qquad \frac{e^2}{(4\pi)^2} \sim \frac{q^4}{\Lambda^4}, \tag{2.2}$$

where q (Λ) refers to a generic low-momentum scale (the pertinent hard scale). Counting rules very similar to the above ones (but not exactly the same) were also used in Refs. [1–3,6–8,14]. The N-nucleon force receives contributions of the order $\sim (q/\Lambda)^\nu$, where

$$\nu = -4 + 2n_\gamma + 2N + 2L + \sum_i V_i \Delta_i. \tag{2.3}$$

Here, L and V_i refer to the number of loops and vertices of type i and n_γ is the number of virtual photons. Further, the vertex dimension Δ_i is given by

$$\Delta_i = d_i + \tfrac{1}{2} n_i - 2, \tag{2.4}$$

where n_i is the number of nucleon field operators and d_i is the q power of the vertex, which accounts for the number of derivatives and insertions of pion mass, ϵ and $e/(4\pi)$ according to Eq. (2.2). Finally, we adopt the counting rule $q/m \sim (q/\Lambda)^2$ for the nucleon mass m, which ensures that all iterations of the leading-order NN potential contribute to the scattering amplitude at leading order $(q/\Lambda)^0$ and thus have to be resumed, see Refs. [15,16] for more details.

Let us now specify the terms in the effective Lagrangian we will need in the present work. It is given in terms of the nucleon isodoublet N and the isovector pion field $\boldsymbol{\pi}$. Utilizing the heavy baryon framework, the relevant isospin-symmetric terms in the effective Lagrangian in the nucleon rest-frame are [17,18]

$$\begin{aligned}
\mathcal{L}^{(0)} &= \frac{1}{2}\partial_\mu \boldsymbol{\pi} \cdot \partial^\mu \boldsymbol{\pi} - \frac{1}{2} M^2 \boldsymbol{\pi}^2 \\
&\quad + N^\dagger \Big[i\partial_0 + \frac{g_A}{2F} \boldsymbol{\tau} \vec{\sigma} \cdot \vec{\nabla} \boldsymbol{\pi} - \frac{1}{4F^2} \boldsymbol{\tau} \cdot (\boldsymbol{\pi} \times \dot{\boldsymbol{\pi}}) \Big] N + \ldots, \\
\mathcal{L}^{(1)} &= N^\dagger \Big[\delta m + 4c_1 M^2 - \frac{2c_1}{F^2} M^2 \boldsymbol{\pi}^2 + \frac{c_2}{F^2} \dot{\boldsymbol{\pi}}^2 + \frac{c_3}{F^2} (\partial_\mu \boldsymbol{\pi} \cdot \partial^\mu \boldsymbol{\pi}) \\
&\quad - \frac{c_4}{2F^2} \epsilon_{ijk} \epsilon_{abc} \sigma_i \tau_a (\nabla_j \pi_b)(\nabla_k \pi_c) \Big] N + \ldots, \qquad (2.5) \\
\mathcal{L}^{(2)} &= N^\dagger \Big[\frac{\vec{\nabla}^2}{2m} + \frac{i g_A}{4mF} \boldsymbol{\tau} \vec{\sigma} \cdot (\overleftarrow{\nabla} \dot{\boldsymbol{\pi}} - \dot{\boldsymbol{\pi}} \overrightarrow{\nabla}) + \frac{2d_{16} - d_{18}}{F} \\
&\quad \times M^2 \boldsymbol{\tau} \vec{\sigma} \cdot \vec{\nabla} \boldsymbol{\pi} + 8 i \tilde{d}_{28} M^2 \partial_0 \Big] N + \ldots,
\end{aligned}$$

where M denotes the pion mass to leading order in quark masses, $M = B(m_u + m_d)$, and F can be identified with the pion decay constant in the chiral limit and with the electromagnetic interactions being switched off. Further, m denotes the physical value of the average nucleon mass, $m = (m_p + m_n)/2$, which is related to the bare mass $\mathring{m}$ via $m = \mathring{m} + \delta m$. Notice that we are using the physical and not the bare nucleon mass in the heavy baryon expansion, see Ref. [19] for more details. This leads to the unusual δm-term in Eq. (2.5). In addition, g_A denotes the axial-vector coupling constant and c_i and d_i ($\tilde{d}_i$) are further low-energy constants (LECs). The relevant isospin-violating part of the Lagrangian reads [1,20–22]

$$\begin{aligned}
\mathcal{L}^{(2)} &= -\frac{e^2}{F^2} C \big(\boldsymbol{\pi}^2 - \pi_3^2 \big) + N^\dagger \Big[2c_5 \epsilon M^2 \tau_3 \\
&\quad - \frac{c_5}{F^2} \epsilon M^2 (\boldsymbol{\pi} \cdot \boldsymbol{\tau}) \pi_3 \Big] N + \ldots, \\
\mathcal{L}^{(3)} &= N^\dagger \Big[f_1 e^2 \big(\pi_3^2 - \boldsymbol{\pi}^2 \big) + \frac{f_2}{2} e^2 F^2 \tau_3 + \frac{f_2}{4} e^2 ((\boldsymbol{\pi} \cdot \boldsymbol{\tau}) \pi_3 \\
&\quad - \boldsymbol{\pi}^2 \tau_3) + \frac{2d_{17} - d_{18} - 2d_{19}}{F} \epsilon M^2 \vec{\sigma} \cdot \vec{\nabla} \pi_3 \Big] N + \ldots, \\
\mathcal{L}^{(4)} &= N^\dagger \Big[\frac{2g_3 + g_4}{4} e^2 F \vec{\sigma} \cdot \vec{\nabla} \pi_3 + \frac{g_4}{4} e^2 F \vec{\sigma} \cdot \vec{\nabla} \pi_3 \tau_3 \\
&\quad + i g_{13} e^2 F^2 (1 + \tau_3) \partial_0 + \frac{4e_{28}}{F} \epsilon M^2 \vec{\sigma} \cdot \vec{\nabla} [\boldsymbol{\tau} \times \dot{\boldsymbol{\pi}}]_3 \\
&\quad + 8 e_{39} \epsilon M^4 \tau_3 \Big] N + \ldots, \qquad (2.6)
\end{aligned}$$

where C, f_i, g_i, and e_i are further LECs. Here, several comments are in order. First, we do not include in Eqs. (2.6) the $e_{38,40}$- and $g_{14,15}$-terms which do not lead to isospin-breaking vertices with no pion fields. Secondly, for the sake of simplicity, we refrain from showing terms with four pion fields in the Lagrangians in Eqs. (2.5), (2.6). The explicit form of such terms is of no relevance for our work. We will, however, briefly discuss these terms in Sec. III A. In addition, we do not show in Eqs. (2.5), (2.6) isospin-violating NN contact interactions, which will be discussed in detail in Sec. III D. Notice further that the complete form of the

[1] Notice that isospin-breaking effects are in general much smaller than indicated by the numerical value of ϵ, because the relevant scale for isospin-conserving contributions is the chiral-symmetry-breaking scale Λ_χ rather than $m_u + m_d$.

[2] Or equivalently, one can use the quark charge matrix $e(1/3 + \tau_3)/2$.

Lagrangian $\mathcal{L}^{(5)}$ has not yet been worked out. We will discuss the relevant structures from $\mathcal{L}^{(5)}$ in Sec. III A. Finally, we do not consider terms with photon fields. Those terms give rise to long-range electromagnetic interactions between two nucleons, which are extensively discussed in Refs. [23–26] and will not be considered in the present work. Notice that the effects of these interactions are enhanced at low energy due to their long range, see, e.g. [27] for more details. In addition to these purely electromagnetic forces, $\pi\gamma$-exchange contributions have to be taken into account at the order $\nu = 4$. The explicit expressions for the corresponding *NN* potential can be found in Ref. [3].

III. ISOSPIN-BREAKING *NN* FORCE

There are many ways to derive nuclear forces from the effective Lagrangian in Eqs. (2.5), (2.6). In this work, we will use the method of unitary transformation [28] which leads to energy-independent and hermitean potentials. Let us first briefly remind the reader of the main idea of this approach. A system of an arbitrary number of interacting pions and nucleons can be completely described by the Schrödinger equation

$$H|\Psi\rangle = E|\Psi\rangle, \tag{3.1}$$

where H denotes the Hamilton operator, which specifies the interaction of pions and nucleons and can be obtained from the Lagrangian using the canonical formalism. Notice that due to the creation of pion field quanta via terms in H, the state Ψ might contain components with an arbitrary number of pions. Instead of solving the above infinite-dimensional equation for few-nucleon system, it is advantageous to project it onto a subspace of the Fock space, that contains only nucleonic states. The resulting equation can be solved using the standard methods of few-body physics. Let η and λ be projection operators on the states $|\phi\rangle$ and $|\psi\rangle$ which satisfy $\eta^2 = \eta$, $\lambda^2 = \lambda$, $\eta\lambda = \lambda\eta = 0$, and $\lambda + \eta = \mathbf{1}$. Equation (3.1) can then be written in the form

$$\begin{pmatrix} \eta H \eta & \eta H \lambda \\ \lambda H \eta & \lambda H \lambda \end{pmatrix} \begin{pmatrix} |\phi\rangle \\ |\psi\rangle \end{pmatrix} = E \begin{pmatrix} |\phi\rangle \\ |\psi\rangle \end{pmatrix}. \tag{3.2}$$

We are now looking for the unitary operator U which has to be chosen in such a way that the transformed Hamilton operator is block-diagonal:

$$\tilde{H} \equiv U^\dagger H U = \begin{pmatrix} \eta \tilde{H} \eta & 0 \\ 0 & \lambda \tilde{H} \lambda \end{pmatrix}. \tag{3.3}$$

In Ref. [28] we have adopted the following ansatz for the operator U:

$$U = \begin{pmatrix} \eta(1 + A^\dagger A)^{-1/2} & -A^\dagger(1 + AA^\dagger)^{-1/2} \\ A(1 + A^\dagger A)^{-1/2} & \lambda(1 + AA^\dagger)^{-1/2} \end{pmatrix}, \tag{3.4}$$

which goes back to the work by Okubo [29]. The operator A in the above equation has only mixed nonvanishing matrix elements: $A = \lambda A \eta$. We stress that the parametrization of the unitary operator U in Eq. (3.4) is not the most general one. The effective Hamilton operator acting on the purely nucleonic subspace of the Fock space can then be obtained via

$$H_{\rm eff} \equiv \eta \tilde{H} \eta = \eta(1 + A^\dagger A)^{-1/2} \left(H + A^\dagger H + HA + A^\dagger H A \right) (1 + A^\dagger A)^{-1/2} \eta. \tag{3.5}$$

The requirement in Eq. (3.3) leads to a set of coupled equations for the operator A, which can be solved perturbatively within the low-momentum expansion along the lines of Ref. [28]. One then ends up with a set of operators that contribute to $H_{\rm eff}$ at a given order in the low-momentum expansion. These operators are constructed out of vertices in the effective Lagrangian and corresponding energy denominators, see Refs. [19,28] for more details. The expressions for the nuclear potential are obtained by evaluating two-nucleon (2*N*), three-nucleon (3*N*), etc., matrix elements of these operators. Let us now be more specific and consider various isospin-violating contributions to the nuclear force up to order $\nu = 5$.

A. One-pion-exchange potential

The isospin-conserving one-pion-exchange (1PE) potential has been studied to one loop in Ref. [19] using both the S-matrix approach, which relies on the standard technique used in quantum field theoretical calculations, and the method of unitary transformation. In that work, we restricted ourselves to isospin-invariant contributions. We now extend this analysis and include isospin-violating corrections to the 1PE potential up to $\nu = 5$. While the main focus of Ref. [19] was to study the quark mass dependence of the nuclear force, here we are only interested in the physically relevant case and do not need to consider the chiral expansion of the various LECs. Thus, there is no need to evaluate explicitly all loop diagrams which lead to pion and nucleon mass and wave-function renormalization as well as to renormalization of the pion-nucleon vertices. In the following, we will explain how to perform the complete calculation of the 1PE potential including renormalization of various LECs within the method of unitary transformation and work out the general structure of the isospin-breaking 1PE potential up to the considered order.

First, we introduce, similar to Ref. [19], renormalized pion fields and masses in the following way:

$$\begin{aligned} \pi_{\rm r}^\pm &= Z_{\pi^\pm}^{-1/2} \pi^\pm, \\ \pi_{\rm r}^0 &= Z_{\pi^0}^{-1/2} \pi^0, \\ Z_{\pi^\pm} &= 1 + \delta Z_\pi, \\ Z_{\pi^0} &= 1 + \delta Z_\pi + \delta \bar{Z}_\pi, \\ M_{\pi^\pm}^2 &= M^2 + \delta M_\pi^2, \\ M_{\pi^0}^2 &= M^2 + \delta M_\pi^2 - \delta \bar{M}_\pi^2. \end{aligned} \tag{3.6}$$

The quantities δZ_π and δM_π^2 denote isospin-invariant contributions to the pion wave function and M_π^2 while $\delta \bar{Z}_\pi$ and $\delta \bar{M}_\pi^2$ represent the corresponding isospin-breaking terms. These quantities can be expanded in powers of the generic low-momentum parameters as follows:

$$\begin{aligned} \delta Z_\pi &= \delta Z_\pi^{(2)} + \delta Z_\pi^{(4)} + \ldots, \\ \delta \bar{Z}_\pi &= \delta \bar{Z}_\pi^{(4)} + \ldots, \\ \delta M_\pi^2 &= \left(\delta M_\pi^2\right)^{(4)} + \left(\delta M_\pi^2\right)^{(6)} + \ldots, \\ \delta \bar{M}_\pi^2 &= \left(\delta \bar{M}_\pi^2\right)^{(4)} + \left(\delta \bar{M}_\pi^2\right)^{(6)} + \ldots, \end{aligned} \tag{3.7}$$

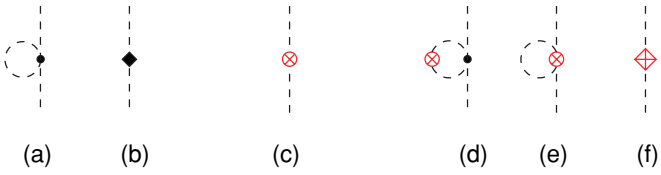

FIG. 1. (Color online) Various contributions to the pion mass and wave function renormalization. Graphs (a) and (b) are the leading isospin-invariant contributions, while the diagrams (c), (d), and (f) show the leading and subleading contributions involving insertions of isospin-violating vertices. Dashed lines refer to pions; solid dots and filled diamonds represent isospin-invariant vertices with $\Delta_i = 0$ and 2 while crossed circles and crossed diamonds denote isospin-breaking vertices of dimension $\Delta_i = 2$ and 4, respectively.

where superscripts correspond to the power of the small parameters according to Eq. (2.2). The leading isospin-invariant corrections $\delta\bar{Z}_\pi^{(2)}$ and $(\delta\bar{M}_\pi^2)^{(4)}$ result from graphs (a) and (b) in Fig. 1 and have already been considered within the method of unitary transformation in Ref. [19]. Leading and subleading isospin-violating contributions are given by diagrams (c) and (d)–(f) in Fig. 1, respectively. The leading contribution to the charged-to-neutral pion mass difference is entirely of electromagnetic origin and given by the C-term in Eq. (2.6):

$$\left(\delta\bar{M}_\pi^2\right)^{(4)} = \frac{2}{F^2}e^2C. \tag{3.8}$$

Here and in what follows, $F_\pi = 92.4$ MeV refers to the measured value of the (charged) pion decay constant.[3] Notice that graph (c) only contributes to the charged-to-neutral pion mass shift and that there are further pion self-energy corrections due to virtual photons, which are not shown explicitly in Fig. 1. The experimentally known pion mass difference $M_{\pi^\pm} - M_{\pi^0} = 4.6$ MeV allows us to fix the value of the LEC C, $C = 5.9 \cdot 10^{-5}$ GeV^4. Notice that the natural scale for this LEC is $F_\pi^2\Lambda^2/(4\pi)^2 \sim 3 \cdot 10^{-5}$ GeV^4 if one adopts $\Lambda \sim M_\rho$. We do not need to explicitly evaluate higher-order corrections to the pion mass and wave function renormalization given by diagrams (d)–(f) in Fig. 1. The relevant contributions are incorporated by using physical values for the charged and neutral pion masses, and the single-pion Hamilton operator expressed in terms of pion creation and destruction operators $a_i^\dagger$ and a_i has the usual form:

$$H_0^\pi = \sum_i \int \frac{d^3k}{(2\pi)^3}\, a_i^\dagger(\vec{k})a_i(\vec{k})\sqrt{\vec{k}^{\,2} + M_i^2}, \tag{3.9}$$

where $M_{1,2} = M_{\pi^\pm}$, $M_3 = M_{\pi^0}$. Notice that at the order considered the effects of the isospin-violating pion wave-function renormalization only shows up via an additional interaction

$$\mathcal{H}^{(4)} = -\frac{g_A\delta Z_\pi}{4F_\pi}N^\dagger\tau_3\,\vec{\sigma}\cdot\vec{\nabla}\pi_3 N, \tag{3.10}$$

which arises from the g_A-vertex being expressed in terms of renormalized pion fields and has the same structure as the g_4-term in Eq. (2.6). Here and in what follows, we will always work with renormalized pion fields and therefore omit the superscript r.

Similar to the pion fields, one can define renormalized proton and neutron fields via $N_p^r = Z_p^{-1/2}N_p$, $N_n^r = Z_n^{-1/2}N_n$. In the isospin symmetric case, the leading contribution to Z_N results from pion loop and the $\tilde{d}_{28}$-term in Eq. (2.5) (for a detailed discussion of wave function renormalization in the heavy baryon approach, see Refs. [30], [31]). Clearly, the NN potential derived using the method of unitary transformation includes contributions from renormalization of external nucleon lines, which, therefore, do not need to be considered separately. Further, we remind the reader that the isospin-invariant nucleon mass shift δm receives contributions at various orders in the low-momentum expansion:

$$\delta m = \delta m^{(1)} + \delta m^{(2)} + \ldots, \qquad \delta m^{(i)} \sim \mathcal{O}\left(\frac{q^{i+1}}{\Lambda^i}\right). \tag{3.11}$$

The leading contribution, $\delta m^{(1)} = -4c_1M_\pi^2$, is clearly due to the second term in the second line of Eq. (2.5) while the subleading one, $\delta m^{(2)}$, receives contributions from pion loops as well as from the counterterms proportional to LECs $f_{1,2,3}$. In addition to isospin-invariant shifts, there are also isospin-breaking shifts $\delta\bar{m}$ to the nucleon mass m_N:

$$m_N \equiv \begin{pmatrix} m_p & 0 \\ 0 & m_n \end{pmatrix} = m + \frac{1}{2}\delta\bar{m}\tau_3. \tag{3.12}$$

The leading and subleading contributions to the proton-to-neutron mass difference are of the strong and electromagnetic origin, respectively:

$$\delta\bar{m}^{(2)} = -4c_5\epsilon M_\pi^2, \qquad \delta\bar{m}^{(3)} = -f_2e^2F_\pi^2. \tag{3.13}$$

At the order we are working, the LECs c_5 and f_2 can be fixed from the strong and electromagnetic shifts to the nucleon mass:

$$\begin{aligned}(m_p - m_n)^{\rm str} &= (\delta\bar{m})^{\rm str} = -2.05 \pm 0.3 \text{ MeV},\\ (m_p - m_n)^{\rm em} &= (\delta\bar{m})^{\rm em} = 0.76 \pm 0.3 \text{ MeV},\end{aligned} \tag{3.14}$$

which leads to [12]

$$c_5 = -0.09 \pm 0.01 \text{ GeV}^{-1}, \qquad f_2 = -0.45 \pm 0.19 \text{ GeV}^{-1}. \tag{3.15}$$

The values for the strong and electromagnetic nucleon mass shifts are taken from Ref. [32]. The electromagnetic shift is based on an evaluation of the Cottingham sum rule which makes use of certain assumptions about the high-energy physics. For a discussion of calculating the neutron-proton mass difference in chiral perturbation theory, see, e.g., Ref. [13] and references therein. We stress that there are further corrections to $\delta\bar{m}$ at higher orders due to pion loop diagrams and counter term insertions. We, however, do not need to consider such higher-order corrections in the present work since we are interested in isospin-violating corrections

[3]The difference between the charged and neutral pion decay constants is $(F_{\pi^\pm} - F_{\pi^0})/F \sim (q/\Lambda)^4$, see, e.g., Ref. [20]. Isospin-breaking effects due to $F_{\pi^\pm} \neq F_{\pi^0}$ in the 1PE potential can be accounted for by small shifts in the pion-nucleon coupling constants as explained below. The corresponding corrections to the 2PE potential enters at order $\nu = 6$ and will not be considered in the present work.

to the NN potential up to order $\nu = 5$. Indeed, since the isospin-invariant 2PE potential starts to contribute at $\nu = 2$, the corrections resulting from insertions of the $\delta\bar{m}^{(2)}$- and $\delta\bar{m}^{(3)}$-vertices start to contribute at orders $\nu = 4$ and $\nu = 5$, respectively. This can easily be verified using Eq. (2.3). As will be shown below, the corrections to the 1PE potential due to the proton-to-neutron mass difference are either proportional to $\delta\bar{m}/m$ or to $(\delta\bar{m})^2$. Consequently, $\delta\bar{m}^{(4)}$ first contributes to the 1PE potential at order $\nu = 6$ which is beyond the scope of the present work. To the order we are working, the single-nucleon Hamilton operator takes the form

$$H_0^N = \sum_{s,t=\pm 1/2} \int \frac{d^3p}{(2\pi)^3}\, n^\dagger_{s,t}(\vec{p}) n_{s,t}(\vec{p}) \left[\frac{\vec{p}^{\,2}}{2m} + t\delta\bar{m}\right], \quad (3.16)$$

where $n^\dagger_{s,t}(\vec{p})$ ($n_{s,t}(\vec{p})$) refers to the creation (destruction) of a nucleon with the spin and isospin quantum numbers s and t and momentum $\vec{p}$, respectively. We stress that further isospin-breaking corrections $\propto \delta\bar{m}/m$ of kinematical origin have to be taken into account in the single-nucleon Hamilton operator entering the Schrödinger equation. For our purposes, however, the expression for H_0^N in Eq. (3.16) is perfectly sufficient. Notice further that here and in what follows, we will not separate the leading and subleading contributions $\delta\bar{m}^{(2)}$ and $\delta\bar{m}^{(3)}$ to the nucleon mass shift: $\delta\bar{m} \simeq \delta\bar{m}^{(2)} + \delta\bar{m}^{(3)}$.

Before going into discussion of various isospin-violating contributions to the 1PE potential, it is instructive to recall its general (i.e., without assuming the isospin limit) form based on the phenomenological pseudovector (PV) Lagrangian $\mathcal{L}_{\rm PV}$ which, for instance, in the case of the neutral pion coupled to protons has the form

$$\mathcal{L}_{\rm PV} = \frac{\sqrt{4\pi}\, f_{pp\pi^0}}{M_{\pi^\pm}} (\bar{N}_p i\gamma_\mu\gamma_5 N_p)\partial^\mu\pi^0. \quad (3.17)$$

Here $f_{pp\pi^0}$ is the corresponding pseudovector coupling constant. Similarly, one can define the coupling constants $f_{nn\pi^0}$, $f_{pn\pi^+}$ and $f_{np\pi^-}$ which correspond to the neutral pion coupled to neutrons and charged pions coupled to nucleons. In the case of exact isospin symmetry these are related to each other via

$$f_{pp\pi^0} = -f_{nn\pi^0} = -\frac{1}{\sqrt{2}} f_{pn\pi^+} = \frac{1}{\sqrt{2}} f_{np\pi^-}. \quad (3.18)$$

Notice that the charged pion mass enters Eq. (3.17) just as a scaling factor in order to make f dimensionless. The 1PE potential can then be expressed in a general form as

$$\begin{aligned} V_{1\pi}(pp) &= f_p^2 V(M_{\pi^0}), \\ V_{1\pi}(nn) &= f_n^2 V(M_{\pi^0}), \\ V_{1\pi}(np) &= -f_0^2 V(M_{\pi^0}) + (-1)^{I+1} 2 f_c^2 V(M_{\pi^\pm}), \end{aligned} \quad (3.19)$$

where we have introduced the constants $f_p^2 = f_{pp\pi^0} f_{pp\pi^0}$, $f_n^2 = f_{nn\pi^0} f_{nn\pi^0}$, $f_0^2 = -f_{pp\pi^0} f_{nn\pi^0}$, and $2f_c^2 = -f_{np\pi^-} f_{pn\pi^+}$. Further, $I = 0, 1$ denotes the total isospin of the two-nucleon system and $V(M_i)$ is defined as

$$V(M_i) = -\frac{4\pi}{M_{\pi^\pm}^2} \frac{(\vec{\sigma}_1\cdot\vec{q}\,)(\vec{\sigma}_2\cdot\vec{q}\,)}{\vec{q}^{\,2} + M_i^2}, \quad (3.20)$$

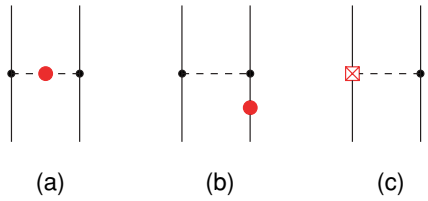

FIG. 2. (Color online) Leading ($\nu = 2$) and subleading ($\nu = 3$) isospin-violating contributions to the 1PE potential. Solid lines refer to nucleons and the crossed rectangle denotes an isospin-violating vertex of dimension $\Delta_i = 3$. A light-shaded circle inserted at a pion or a nucleon line refers to a single insertion of $\delta\bar{M}_\pi^2$ or $\delta\bar{m}^{(2)} + \delta\bar{m}^{(3)}$, correspondingly. Diagrams which result from the interchange of the nucleon lines and from the application of the time reversal operation are not shown. For remaining notation see Fig. 1.

where we use the static approximation for nucleons and neglect all relativistic corrections. Charge symmetry implies the same interaction in the pp and nn case, i.e., $f_{pp\pi^0} = -f_{nn\pi^0}$ or $f_p^2 = f_n^2 = f_0^2$. In case of charge independence, one has $f_p^2 = f_n^2 = f_0^2 = f_c^2 \equiv f^2$. The coupling constant f^2 is related to the nucleon axial vector coupling g_A via

$$f^2 = \frac{1}{4\pi}\left[\frac{g_A M_{\pi^\pm}}{2F_\pi}(1+\delta)\right]^2, \quad (3.21)$$

where δ denotes an isospin-conserving Goldberger-Treiman discrepancy.[4] In the general case when isospin symmetry is not conserved, we can introduce in a close analogy to Ref. [2] the quantities δ_p, δ_n, and δ_c corresponding to f_p^2, f_n^2, and f_c^2, respectively. It is sufficient to know the values of these three constants δ_p, δ_n, and δ_c in order to determine completely the expressions for the 1PE potential in Eqs. (3.19), since the coupling constant f_0^2 can be expressed as

$$f_0^2 = \frac{1}{4\pi}\left[\frac{g_A M_{\pi^\pm}}{2F_\pi}\right]^2 (1+\delta_p)(1+\delta_n). \quad (3.22)$$

Notice that the dominant contribution to the Goldberger-Treiman discrepancy is generated by the d_{18}-term in Eq. (2.5) and does not beak isospin symmetry:

$$\delta_p^{(2)} = \delta_n^{(2)} = \delta_c^{(2)} = -\frac{2M_\pi^2}{g_A} d_{18}. \quad (3.23)$$

In what follows, we will use the convenient form of the 1PE potential given in Eqs. (3.19) which already incorporates the dominant isospin-breaking effects due to the pion-mass difference and charge dependence of the pion-nucleon coupling constant.

We are now in the position to discuss the isospin-violating 1PE potential. The leading and subleading contributions at orders $\nu = 2$ and $\nu = 3$ are shown in Fig. 2. Since we use $\delta\bar{m}$ and are not separating $\delta\bar{m}^{(2)}$ and $\delta\bar{m}^{(3)}$, graph (b) in Fig. 2 contains both the order $\nu = 2$ and $\nu = 3$ contributions to the

[4]The Goldberger-Treiman discrepancy is defined in terms of pseudoscalar coupling constant g. Pseudoscalar and pseudovector couplings lead to the same expression for the 1PE potential on-energy-shell provided the coupling constants are related via $f = gM_{\pi^\pm}/(2m)$.

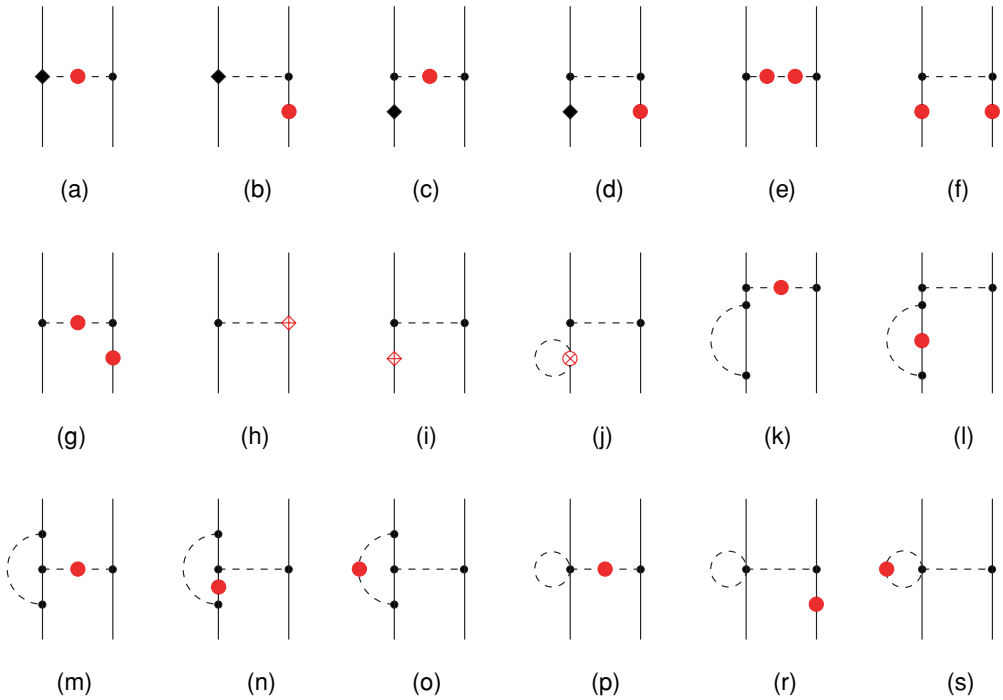

FIG. 3. (Color online) Order $\nu = 4$ contributions to the 1PE potential which contain isospin-violating vertices. For diagrams with insertions of the nucleon mass shift only one representative topology is depicted. Further graphs with nucleon mass insertions at different internal or external nucleon lines are not shown. For remaining notation, see Figs. 1 and 2.

1PE potential. Using the method of unitary transformation introduced above and utilizing the notation of Refs. [9,33], one finds the following result for diagrams (a) and (b) in Fig. 2:

$$V_{1\pi} = -\frac{1}{2}\eta'\left[H^{(0)}\frac{\lambda^1}{(H_0 - E_\eta)}H^{(0)} + H^{(0)}\frac{\lambda^1}{(H_0 - E_{\eta'})}H^{(0)}\right]\eta, \tag{3.24}$$

where η and η' denote the projectors on the purely nucleonic subspace of the Fock space, while λ^i refers to the projector on the states with i pions. Further, $H^{(0)}$ is the leading isospin-invariant πNN vertex proportional to g_A, H_0 denotes the single-particle Hamilton operator, $H_0 = H_0^\pi + H_0^N$, and E_η ($E_{\eta'}$) refers to the energy of the nucleons in the state η (η'). The contribution of graph (a) to the 1PE potential can be obtained by evaluating the corresponding matrix element of the operator $V_{1\pi}$ in Eq. (3.24) in the limits $m \to \infty$ and $\delta\bar{m} \to 0$. Clearly, this contribution is already included in Eqs. (3.19). Similarly, the contribution of the diagram (b) is obtained by evaluating the matrix element in the limits $m \to \infty$ and $\delta\bar{M}_\pi^2 \to 0$ and expanding energy denominators in powers of $\delta\bar{m}$. The term linear in $\delta\bar{m}$ leads to vanishing matrix elements, so that there is no contribution from graph (b) to the 1PE potential. Finally, the contribution of the last diagram (c) can be obtained by evaluating the matrix elements of the operator

$$V_{1\pi} = -\frac{1}{2}\eta'\left[H^{(0)}\frac{\lambda^1}{(H_0 - E_\eta)}H^{(3)} + H^{(0)}\frac{\lambda^1}{(H_0 - E_{\eta'})}H^{(3)}\right]\eta + \text{h.c.}, \tag{3.25}$$

in the limits $m \to \infty$, $\delta\bar{m} \to 0$ and $\delta\bar{M}_\pi^2 \to 0$. Here, $H^{(3)}$ denotes an isospin-violating vertex from the Lagrangian $\mathcal{L}^{(3)}$ in Eq. (2.6) which is proportional to the combination of the LECs $2d_{17} - d_{18} - 2d_{19}$. It provides a contribution to the quantities δ_p and δ_n [2]:

$$\delta_p^{(3)} = -\delta_n^{(3)} = 2\frac{2d_{17} - d_{18} - 2d_{19}}{g_A}\epsilon M_\pi^2, \tag{3.26}$$

which leads to the charge-symmetry breaking 1PE potential.

Isospin-violating contributions to the 1PE potential at order $\nu = 4$ are depicted in Fig. 3. Notice that pion tadpole graphs with the Weinberg-Tomozawa vertex lead to vanishing contributions and are not shown in Fig. 3. In addition, pion loop diagrams (but not of the tadpole type) with one insertion of the Weinberg-Tomozawa or c_5-vertex do not contribute since only odd functions of the loop momentum enter the corresponding integrals. We do not show those diagrams in Fig. 3 either. Finally, we also ignore one-loop nucleon self-energy contributions with insertions of the pion mass difference, since they do not lead to isospin-violating contributions. Let us begin with the first graph (a) in Fig. 3. The contribution proportional to d_{16} leads to renormalization of the nucleon axial vector coupling constant g_A while the one proportional to d_{18} provides a dominant contribution to the isospin-conserving Goldberger-Treiman discrepancy, see Eq. (3.26). Further, the leading relativistic $1/m$-correction vanishes as does the corresponding isospin-invariant contribution. This can easily be understood in terms of Feynman diagrams. Indeed, the $1/m$-vertex in the last line of Eq. (2.5) contains a time derivative of the pion field. Since the four-momentum is

conserved, it gives a contribution proportional to the nucleon kinetic energy which is of the order $\nu = 6$. For graph (b) we find that the contributions proportional to d_{16} and d_{18} vanish. The leading relativistic correction $\propto \delta\bar{m}/m$ corresponding to this diagram can be obtained by evaluating matrix elements of the operators in Eq. (3.25), where $H^{(3)}$ corresponds now to the second term in the last line of Eq. (2.5). Taking the limit $m \to \infty$ in Eq. (3.16), expanding the energy denominators in powers of $\delta\bar{m}$ and keeping only terms linear in $\delta\bar{m}$, we find

$$V_{1\pi}^{3b} = i\frac{\delta\bar{m}}{2m}\left(\frac{g_A}{2F_\pi}\right)^2 [\boldsymbol{\tau}_1\times\boldsymbol{\tau}_2]_3 \frac{1}{\left(\vec{q}_1^{\,2}+M_\pi^2\right)}[(\vec{\sigma}_1\cdot\vec{q}_1)(\vec{\sigma}_2\cdot(\vec{p}_2 + \vec{p}_2')) + (\vec{\sigma}_1\cdot(\vec{p}_1+\vec{p}_1'))(\vec{\sigma}_2\cdot\vec{q}_1)], \tag{3.27}$$

where $\vec{p}_i$ ($\vec{p}_i'$) denotes the incoming (outgoing) momentum of the nucleon i and $\vec{q}_1 = \vec{p}_1' - \vec{p}_1 = -(\vec{p}_2' - \vec{p}_2)$. The order $\Delta_i = 2$ isospin-invariant interaction in the next two graphs (c) and (d) is due to the $\tilde{d}_{28}$-vertex, $\delta m^{(2)}$ and the nucleon kinetic energy. The $\tilde{d}_{28}$-term in the Lagrangian is proportional to the nucleon equation of motion and is only needed for renormalization purpose.[5] In the method of unitary transformation, this term is eliminated from the Lagrangian by an appropriate field redefinition, see Ref. [19] for more details. The contributions from graphs (c) and (d) proportional to the nucleon kinetic energy can be obtained evaluating matrix elements of the operators in Eq. (3.24), expanding in $\delta\bar{M}_\pi^2, 1/m$ and $\delta\bar{m}$ and keeping only terms proportional to $\delta\bar{M}_\pi^2/m$ and $\delta\bar{m}/m$, respectively. We find that graph (c) leads to a vanishing result while graph (d) provides the following contribution to the 1PE potential:

$$V_{1\pi}^{3d} = -i\frac{\delta\bar{m}}{2m}\left(\frac{g_A}{2F_\pi}\right)^2 [\boldsymbol{\tau}_1\times\boldsymbol{\tau}_2]_3 \frac{(\vec{\sigma}_1\cdot\vec{q}_1)(\vec{\sigma}_2\cdot\vec{q}_1)}{\left(\vec{q}_1^{\,2}+M_\pi^2\right)^2} \times\left(\vec{p}_1^{\,2}-\vec{p}_2^{\,2}-\vec{p}_1'^2+\vec{p}_2'^2\right). \tag{3.28}$$

Introducing the total momentum $\vec{P}$ of the two-nucleon system, $\vec{P} = \vec{p}_1 + \vec{p}_2 = \vec{p}_1' + \vec{p}_2'$, the above expression can be rewritten as

$$V_{1\pi}^{3d} = i\frac{\delta\bar{m}}{m}\left(\frac{g_A}{2F_\pi}\right)^2 [\boldsymbol{\tau}_1\times\boldsymbol{\tau}_2]_3 \frac{(\vec{\sigma}_1\cdot\vec{q}_1)(\vec{\sigma}_2\cdot\vec{q}_1)}{\left(\vec{q}_1^{\,2}+M_\pi^2\right)^2}\vec{q}_1\cdot\vec{P}. \tag{3.29}$$

Thus, this potential vanishes in the two-nucleon center of mass (c.m.). The contributions from graphs (c) and (d) proportional to $\delta m^{(2)}$ are found to vanish. As pointed out before, the contribution from diagram (e) in Fig. 3 proportional to $(\delta\bar{M}_\pi^2)^2$ is already taken into account in Eqs. (3.19). For graph (f) we obtain the following contribution to the 1PE potential, see also Refs. [1,8,34]:

$$V_{1\pi}^{3f} = -(\delta\bar{m})^2\left(\frac{g_A}{2F_\pi}\right)^2 \left(\boldsymbol{\tau}_1\cdot\boldsymbol{\tau}_2 - \tau_1^3\tau_2^3\right)\frac{(\vec{\sigma}_1\cdot\vec{q})(\vec{\sigma}_2\cdot\vec{q})}{\left(\vec{q}^{\,2}+M_\pi^2\right)^2}. \tag{3.30}$$

[5]It absorbs the ultraviolet divergence in the nucleon Z-factor calculated to one loop.

Notice that the isospin-violating piece has the same structure as the correction due to the pion mass difference at order $\nu = 2$ but is $\delta\bar{M}_\pi^2/(\delta\bar{m})^2 \sim 660$ times weaker. Next, graph (g) is expected to provide a correction proportional to $\delta\bar{m}\delta\bar{M}_\pi^2$. We find that the corresponding contribution vanishes. Further, the contribution of diagram (h) is included in the 1PE potential in Eqs. (3.19), where one has to account for shifts in the pion-nucleon coupling constants:

$$\delta f_p^{(4)} = \frac{g_3+g_4}{g_A}e^2F_\pi^2 + \frac{\delta Z_\pi}{2}, \quad \delta f_n^{(4)} = -\frac{g_3}{g_A}e^2F_\pi^2 + \frac{\delta Z_\pi}{2}. \tag{3.31}$$

Consider now diagram (i) in Fig. 3. The isospin-violating counterterms of dimension $\Delta_i = 4$ include both the strong term $\propto e_{39}$ which leads to the nucleon mass shift, and the electromagnetic one $\propto g_{13}$ which is proportional to the nucleon equation of motion and absorbs the ultraviolet divergence in the nucleon Z-factor. We find that this diagram as well as *all* remaining diagrams (j)–(s) in Fig. 3 either lead to vanishing contributions or renormalize various LECs. In particular, contributions of graphs (k) and (i), (j), (l) can be expressed in terms of isospin-conserving and isospin-violating nucleon self-energy corrections, while diagrams (m), (p), (r) and (n), (o), (s) give rise to isospin-invariant and isospin-breaking renormalization of the pion-nucleon coupling constants. None of the pion loop diagrams lead to any form-factor-like behavior, i.e., have a nontrivial dependence on the momentum transfer between two nucleons. Thus the contribution of all these diagrams is taken into account by using the general expressions for the one-pion exchange potential in Eqs. (3.19) expressed in terms of renormalized quantities. Stated differently, the contributions of these diagrams only lead to charge-dependent shifts in the strength of the 1PE potential. We stress that since the corresponding LECs $g_3^{\rm r}$ and $g_4^{\rm r}$ are not known experimentally and have to be determined from the data, and because we are not interested in the quark-mass dependence of the strength of the 1PE potential, we do not need to evaluate the loop diagrams in Fig. 3 explicitly. Finally, we have also verified the finding of Ref. [2], that the contributions of diagrams (l) and (n) cancel.

Let us now discuss the corrections to the 1PE potential at order $\nu = 5$ represented by the diagrams depicted in Fig. 4. Notice that we again refrain from showing various kinds of diagrams which lead to vanishing contributions as explained above. For the same reason, we also do not show graphs with an insertion of the $\pi\pi NN$ vertices proportional to f_1, f_2 (but not of the tadpole type) as well as pion tadpole diagrams proportional to c_i with an insertion of the $\delta\bar{M}_\pi^2$-vertex at the pion line, which do not lead to isospin-violating contributions to the potential. First, we note that the contribution of graph (a) proportional to the LECs d_{16} and d_{18} is already included in Eqs. (3.19). Further, similar to the case of diagram (a) in Fig. 3, the corresponding $1/m$-correction vanishes at this order. Diagrams (b) and (c) also do not lead to new structures in the 1PE potential: the term $\propto \tilde{d}_{28}$ provides a shift of the strength of the charge-symmetry-breaking (CSB) 1PE potential via the nucleon wave-function renormalization while the contributions proportional to the nucleon kinetic energy

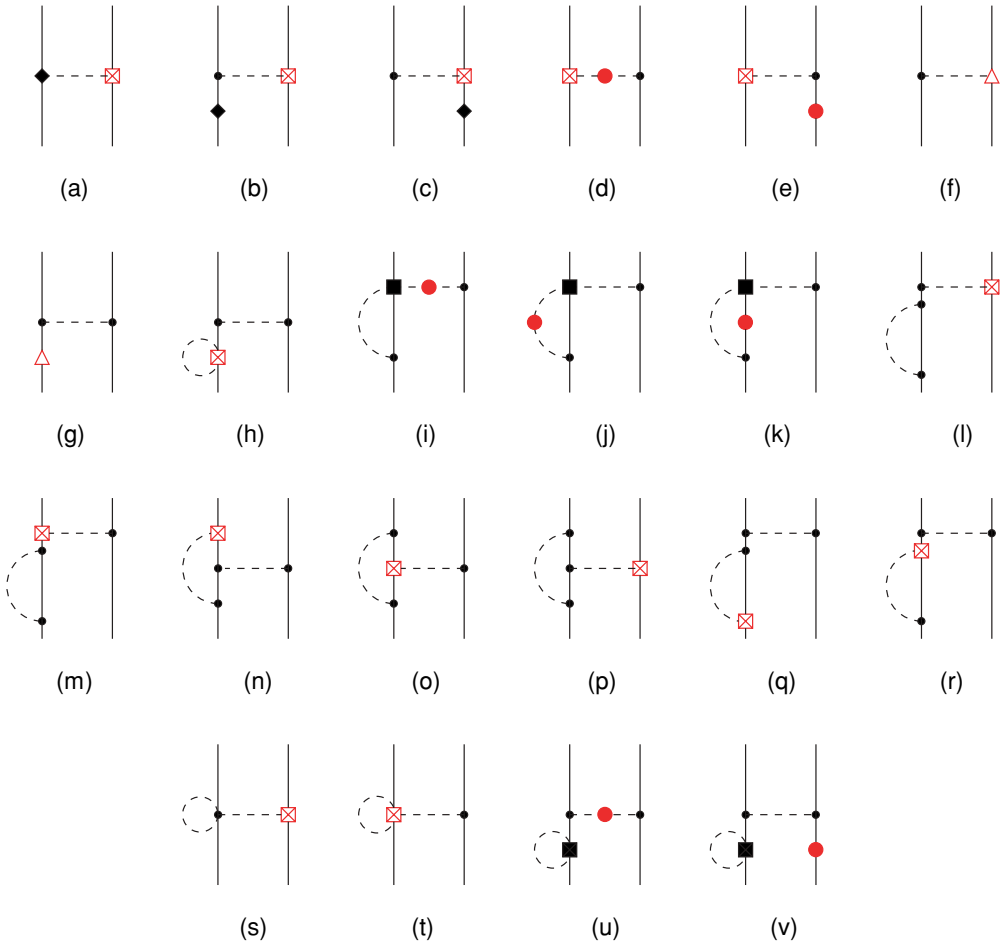

FIG. 4. (Color online) Order $\nu = 5$ contributions to the 1PE potential which contain isospin-violating vertices. Filled rectangles refer to isospin-invariant vertices of dimension $\Delta_i = 1$ while triangles denote isospin-breaking interactions of dimension $\Delta_i = 5$. For remaining notation, see Figs. 1, 2, 3.

and to $\delta m^{(2)}$ vanish. Similarly, diagrams of the type (c) and (d) in Fig. 3 but proportional to $\delta m^{(3)}$ instead of $\delta m^{(2)}$, which are not shown explicitly in Fig. 4, lead to a vanishing result. The contribution of diagram (d) is already included in the expression for the 1PE potential in Eqs. (3.19). Graph (e) leads to a vanishing result. Consider now the contribution of diagram (f). Order $\Delta_i = 5$ isospin-violating counter terms have not yet been worked out. Here we simply list all possible structures consistent with the usual symmetry constraints:

$$\mathcal{L}^{(5)} = N^\dagger \big(a e^2 \vec{\sigma} \cdot \vec{\nabla} [\boldsymbol{\tau} \times \dot{\boldsymbol{\pi}}]_3 + b_1 \epsilon M_\pi^2 \vec{\sigma} \cdot \vec{\nabla} \vec{\nabla}^2 \pi_3 + b_2 \epsilon M_\pi^2 \vec{\sigma} \cdot \vec{\nabla} \ddot{\pi}_3 + b_3 \epsilon M_\pi^4 \vec{\sigma} \cdot \vec{\nabla} \pi_3 \big) N, \quad (3.32)$$

where a and b_i are LECs. The first term in the above expression does not contribute at order $\nu = 5$ due to the presence of the time derivative. The 1PE potential proportional to b_i can be cast into the form of Eqs. (3.19) plus additional CSB short-range interactions. Further, one has to take into account relativistic $1/m$-terms

$$\mathcal{L}^{(5)} = i \frac{2d_{17} - d_{18} - 2d_{19}}{2m F_\pi} \epsilon M_\pi^2 \, N^\dagger \vec{\sigma} \cdot \big(\overleftarrow{\nabla} \dot{\pi}_3 - \dot{\pi}_3 \overrightarrow{\nabla} \big) N, \quad (3.33)$$

which, however, contribute at higher orders due to the presence of the time derivative. Graph (g) in Fig. 4 represents the correction to the 1PE potential due to an insertion of the order $\Delta_i = 5$ isospin-violating counter terms. To the best of our knowledge, the latter have not yet been worked out. They may include ϵM_π^4-terms proportional to the nucleon equation of motion which contribute to the nucleon Z-factor as well as terms $\propto M_\pi^2 e^2/(4\pi)^2$ which give further corrections to the nucleon mass difference. Again, we do not need to evaluate explicitly the contributions of this diagram as well as all remaining graphs (h)–(v) in Fig. 4 since they do not lead to any new structures in the 1PE potential. We have verified that diagrams of type (k) only lead to shifts in the pion-nucleon coupling constants δ_i. We further note that the loop integral in graph (j) has no logarithmic ultraviolet divergence, which is consistent with the fact that diagram (f) has no contribution due to counter terms of electromagnetic origin.

To summarize, isospin-violating corrections to the 1PE potential up to $\nu = 5$ are accounted for by using the expression in Eqs. (3.19) and further corrections in Eqs. (3.27), (3.28), and (3.30). The CSB corrections in Eqs. (3.27) and (3.28) obtained within the method of unitary transformation agree with the ones found in Ref. [8] using a completely different

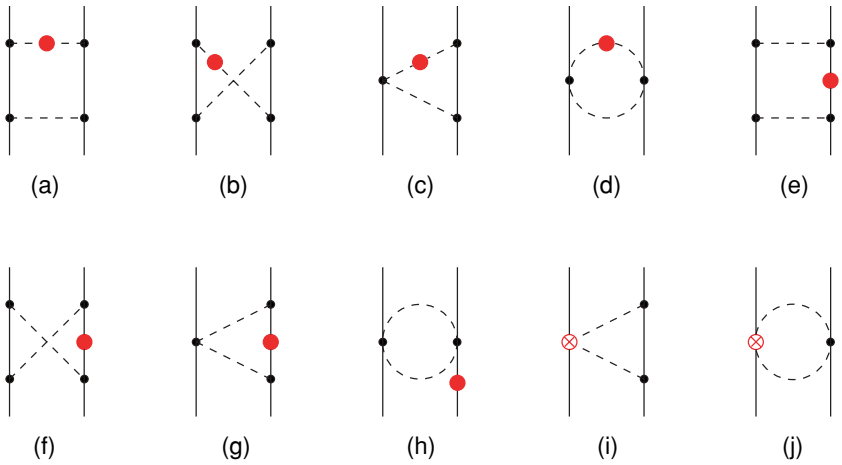

FIG. 5. (Color online) Leading isospin-breaking correction to the 2PE potential at order $\nu = 4$. For notation, see Figs. 1, 2, and 3.

framework. The correction $\propto (\delta\bar{m})^2$ in Eq. (3.30) can be found, e.g., in Ref. [34], see also discussion in Ref. [8].

B. Two-pion-exchange potential

Let us now discuss the leading and subleading isospin-violating two-pion-exchange potential which can be expressed in momentum space as

$$V_{2\pi} = \left(\tau_1^3\tau_2^3\right)[V_C + V_S(\vec{\sigma}_1\cdot\vec{\sigma}_2) + V_T(\vec{\sigma}_1\cdot\vec{q})(\vec{\sigma}_2\cdot\vec{q})] + \left(\tau_1^3+\tau_2^3\right)[W_C + W_S(\vec{\sigma}_1\cdot\vec{\sigma}_2) + W_T(\vec{\sigma}_1\cdot\vec{q})(\vec{\sigma}_2\cdot\vec{q})], \tag{3.34}$$

with the six functions $V_C(q),\ldots,W_T(q)$ depending on the momentum transfer $q \equiv |\vec{q}|$. The subscripts refer to the central (C), spin-spin (S), and tensor (T) components in the potential. Further, V_i and W_i correspond to charge-symmetry conserving and charge-symmetry breaking pieces, respectively. The dominant contributions arise at order $\nu = 4$ from diagrams shown in Fig. 5. In this figure, graphs (a)–(d) represent the effects due to the pion mass difference, graphs (e)–(h) provide contributions proportional to the nucleon mass difference, and the last two graphs (i) and (j) are due to a single insertion of the isospin-breaking $\pi\pi NN$-vertex proportional to the LEC c_5.

The isospin-violating two-pion-exchange (2PE) potential due to the pion mass difference has been considered in Ref. [6]. As shown in this reference, it can be expressed in terms of the corresponding isospin-invariant contributions without performing any additional calculations. To that aim, one can first decompose the isospin-invariant 2PE potential into the isoscalar and isovector pieces

$$V_{2\pi} = V_{2\pi}^0 + V_{2\pi}^1\boldsymbol{\tau}_1\cdot\boldsymbol{\tau}_2. \tag{3.35}$$

The leading isospin-breaking effects die to $M_{\pi^\pm} \neq M_{\pi^0}$ are incorporated properly if one uses $\tilde{M}_\pi$, defined as

$$\tilde{M}_\pi = \tfrac{2}{3}M_{\pi^\pm} + \tfrac{1}{3}M_{\pi^0}, \tag{3.36}$$

in the scalar part $V_{2\pi}^0$ and expresses the vector part as following:

$$V_{2\pi}^1 = \begin{cases} V_{2\pi}^1(M_{\pi^\pm}) & \text{for} \quad pp \text{ and } nn, \\ V_{2\pi}^1(M_{\pi^0}) & \text{for} \quad np, \quad T=1, \\ V_{2\pi}^1(\tilde{M}_\pi) & \text{for} \quad np, \quad T=0. \end{cases} \tag{3.37}$$

These results are valid modulo $(\delta\bar{M}_\pi^2/M_\pi^2)^2$-corrections. Notice that terms $\propto (\delta\bar{M}_\pi^2/M_\pi^2)^2$ start to contribute to the 2PE potential at order $\nu = 6$ and thus need not be considered in the present work. Equivalently, we can write the 2PE potential in the form

$$V_{2\pi} = V_{2\pi}^0(\tilde{M}_\pi) + V_{2\pi}^1(\bar{M}_\pi)\,\boldsymbol{\tau}_1\cdot\boldsymbol{\tau}_2 + \frac{\delta\bar{M}_\pi^2}{4M_\pi}\times\frac{\partial V_{2\pi}^1(M_\pi)}{\partial M_\pi}\,\tau_1^3\tau_2^3 + \mathcal{O}\left(\left(\frac{\delta M_\pi^2}{M_\pi^2}\right)^2\right), \tag{3.38}$$

where $\bar{M}_\pi$ is the average pion mass

$$\bar{M}_\pi = \tfrac{1}{2}(M_{\pi^\pm} + M_{\pi^0}). \tag{3.39}$$

Substituting the expressions for the isospin-invariant 2PE potential at $\nu = 2$ given, e.g., in Ref. [35] into Eq. (3.38) we obtain for the nonpolynomial parts of the contribution of diagrams (a)–(d) in Fig. 5:

$$V_C^{(4)} = \frac{\delta\bar{M}_\pi^2}{128\pi^2F_\pi^4}\frac{1}{4M_\pi^2+q^2}\left\{4g_A^4M_\pi^2 - \left(4M_\pi^2\left(9g_A^4-4g_A^2-1\right) + q^2\left(11g_A^4-6g_A^2-1\right) - \frac{16g_A^4M_\pi^4}{4M_\pi^2+q^2}\right)L^\Lambda(q)\right\}, \tag{3.40}$$

where the loop function $L^\Lambda(q)$ reads

$$L^\Lambda(q) = \frac{\omega}{2q}\ln\frac{\Lambda^2\omega^2 + q^2s^2 + 2\Lambda q\omega s}{4M_\pi^2(\Lambda^2+q^2)}, \qquad \omega = \sqrt{q^2+4M_\pi^2}, \qquad s = \sqrt{\Lambda^2-4M_\pi^2}. \tag{3.41}$$

The above expression for $L^\Lambda(q)$ is given in the spectral-function regularization (SFR) framework with Λ being the corresponding cutoff. The limit $\Lambda\to\infty$ corresponds to dimensional regularization (DR).

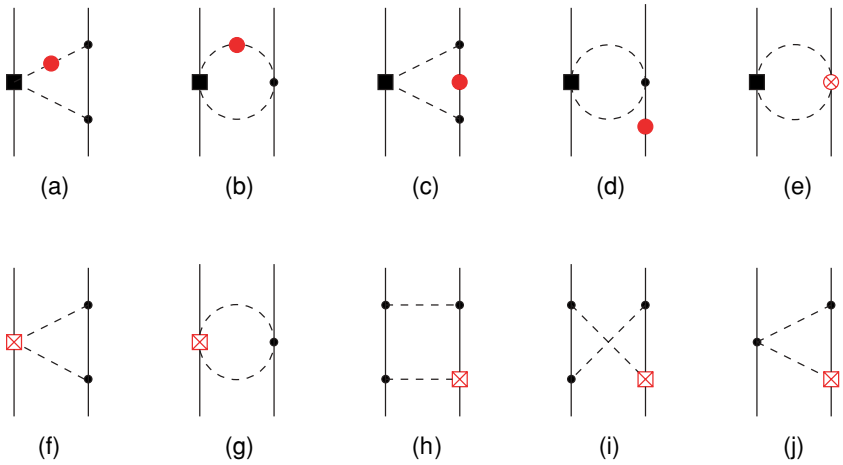

FIG. 6. (Color online) Subleading isospin-breaking correction to the 2PE potential at order $\nu = 5$. For notation see Figs. 1–4.

Consider now diagrams (e)–(h) in Fig. 5 which include one insertion of the nucleon mass shift. The contributions of graphs (e) and (f) can be obtained within the method of unitary transformation by evaluating the corresponding matrix elements of the operator

$$
\begin{aligned}
V_{2\pi}^{5e,5f} &= \eta'\Bigg[\frac{1}{2}H^{(0)}\frac{\lambda^1}{(H_0-E_{\eta'})}H^{(0)}\tilde{\eta}H^{(0)}\frac{\lambda^1}{(H_0-E_{\tilde{\eta}})(H_0-E_{\eta'})}H^{(0)} \\
&\quad -\frac{1}{8}H^{(0)}\frac{\lambda^1}{(H_0-E_{\eta'})}H^{(0)}\tilde{\eta}H^{(0)}\frac{\lambda^1}{(H_0-E_{\tilde{\eta}})(H_0-E_{\eta})}H^{(0)} \\
&\quad +\frac{1}{8}H^{(0)}\frac{\lambda^1}{(H_0-E_{\eta'})(H_0-E_{\tilde{\eta}})}H^{(0)}\tilde{\eta}H^{(0)}\frac{\lambda^1}{(H_0-E_{\tilde{\eta}})}H^{(0)} \\
&\quad -\frac{1}{2}H^{(0)}\frac{\lambda^1}{(H_0-E_{\eta})}H^{(0)}\frac{\lambda^2}{(H_0-E_{\eta})}H^{(0)} \\
&\quad \times\frac{\lambda^1}{(H_0-E_{\eta})}H^{(0)}\Bigg]\eta + \text{h.c.}
\end{aligned}
\tag{3.42}
$$

in the limits $m \to \infty$, $\delta\bar{M}_\pi^2 \to 0$ by expanding the denominators in powers of $\delta\bar{m}$ and keeping only terms linear in $\delta\bar{m}$.[6] Similarly, contributions of diagrams (g) and (h) can be obtained by evaluating the matrix elements of the operators

$$
\begin{aligned}
V_{2\pi}^{5g} &= \frac{1}{2}\eta'\Bigg[H^{(0)}\frac{\lambda^1}{(H_0-E_{\eta})}H^{(0)}\frac{\lambda^2}{(H_0-E_{\eta})}H^{(0)} \\
&\quad +H^{(0)}\frac{\lambda^2}{(H_0-E_{\eta})}H^{(0)}\frac{\lambda^1}{(H_0-E_{\eta})}H^{(0)} \\
&\quad +H^{(0)}\frac{\lambda^1}{(H_0-E_{\eta})}H^{(0)}\frac{\lambda^1}{(H_0-E_{\eta})}H^{(0)}\Bigg]\eta + \text{h.c.},
\end{aligned}
\tag{3.43}
$$

and

$$
V_{2\pi}^{5h} = \frac{1}{2}\eta'\Bigg[H^{(0)}\frac{\lambda^2}{(H_0-E_{\eta'})}H^{(0)} + H^{(0)}\frac{\lambda^2}{(H_0-E_{\eta})}H^{(0)}\Bigg]\eta,
\tag{3.44}
$$

respectively. Finally, the operators corresponding to the last two graphs in Fig. 5 read

$$
\begin{aligned}
V_{2\pi}^{5i} &= \eta'\Bigg[H^{(0)}\frac{\lambda^1}{\omega}H^{(0)}\frac{\lambda^2}{(\omega_1+\omega_2)}H^{(2)} \\
&\quad +H^{(2)}\frac{\lambda^2}{(\omega_1+\omega_2)}H^{(0)}\frac{\lambda^1}{\omega}H^{(0)} + H^{(0)}\frac{\lambda^1}{\omega}H^{(2)}\frac{\lambda^1}{\omega}H^{(0)}\Bigg]\eta,
\end{aligned}
\tag{3.45}
$$

and

$$
V_{2\pi}^{5j} = \eta'\Bigg[H^{(2)}\frac{\lambda^2}{(\omega_1+\omega_2)}H^{(0)} + H^{(0)}\frac{\lambda^2}{(\omega_1+\omega_2)}H^{(2)}\Bigg]\eta,
\tag{3.46}
$$

where the ω's refer to the pionic free energy in the isospin limit and $H^{(2)}$ denotes the isospin-violating $\pi\pi NN$ vertex from the Lagrangian $\mathcal{L}^{(2)}$ proportional to the LEC c_5. Performing a straightforward evaluation of the matrix elements of these operators, we obtain the following result for the leading CSB 2PE potential:

$$
\begin{aligned}
W_C^{(4)} &= -\frac{g_A^2}{64\pi F_\pi^4}\Bigg\{\frac{2g_A^2\delta\bar{m}M_\pi^3}{4M_\pi^2+q^2} \\
&\quad -\left(4g_A^2\delta\bar{m}-(\delta\bar{m})^{\text{str}}\right)\left(2M_\pi^2+q^2\right)A^\Lambda(q)\Bigg\}, \\
W_T^{(4)} &= -\frac{1}{q^2}W_S^{(4)} = \frac{g_A^4\delta\bar{m}}{32\pi F_\pi^4}A^\Lambda(q),
\end{aligned}
\tag{3.47}
$$

where the loop function $A^\Lambda(q)$ is given by

$$
A^\Lambda(q) = \frac{1}{2q}\arctan\frac{q(\Lambda-2M_\pi)}{q^2+2\Lambda M_\pi}.
\tag{3.48}
$$

Here, several comments are in order. First, one should keep in mind that we again only show explicitly the nonpolynomial terms. Secondly, we found that the planar box graph (e) and the "football" diagrams (h) and (j) lead to vanishing contributions. Notice further that we have also included the order $\nu = 5$ contribution from graph (f) in Fig. 6. The latter is proportional to the LEC f_2 or, equivalently, to $(\delta\bar{m})^{\text{em}}$ and has the same structure as the contribution of diagram (i) in Fig. 5 which is $\propto c_5$ or, equivalently, $\propto (\delta\bar{m})^{\text{str}}$. It is therefore convenient to combine these contributions and to express them in terms of,

[6]Notice that the contribution $\propto \delta\bar{M}_\pi$ discussed above can also be obtained from Eq. (3.42) if one takes the limits $m \to \infty$, $\delta\bar{m} \to 0$ in H_0.

e.g., $\delta\bar{m}$ and $(\delta\bar{m})^{\rm str}$. Finally, we would like to emphasize that the result given in Eq. (3.47) agrees with previous calculations, see Refs. [7,36] and [37] for related older work.

Consider now the subleading isospin-breaking two-pion-exchange potential generated by diagrams shown in Fig. 6. First, charge-symmetry conserving contributions from graphs (a) and (b) due to the pion mass difference can be obtained using Eq. (3.38) from the corresponding isospin-invariant 2PE potential. We find

$$V_T^{(5)} = -\frac{1}{q^2} V_S^{(5)} = -\frac{\delta\bar{M}_\pi^2}{16\pi F_\pi^4}\, g_A^2 c_4 A^\Lambda(q). \qquad (3.49)$$

The contributions of graphs (c) and (d) result in the method of unitary transformation from the operators

$$V_{2\pi}^{\rm 6c} = \frac{1}{2}\eta'\Big[H^{(0)}\frac{\lambda^1}{(H_0-E_\eta)}H^{(0)}\frac{\lambda^2}{(H_0-E_\eta)}H^{(1)} + H^{(1)}\frac{\lambda^2}{(H_0-E_\eta)}H^{(0)}\frac{\lambda^1}{(H_0-E_\eta)}H^{(0)} + H^{(0)}\frac{\lambda^1}{(H_0-E_\eta)}H^{(1)}\frac{\lambda^1}{(H_0-E_\eta)}H^{(0)}\Big]\eta + \text{h.c.}, \qquad (3.50)$$

and

$$V_{2\pi}^{\rm 6d} = \frac{1}{2}\eta'\Big[H^{(1)}\frac{\lambda^2}{(H_0-E_{\eta'})}H^{(0)} + H^{(1)}\frac{\lambda^2}{(H_0-E_\eta)}H^{(0)}\Big]\eta + \text{ h.c.}, \qquad (3.51)$$

where $H^{(1)}$ refers to $\pi\pi NN$ vertices from $\mathcal{L}^{(1)}$ proportional to c_i. Further, contributions from graphs (e) and (g) in Fig. 6 can be obtained from $V_{2\pi}^{\rm 5j}$ in Eq. (3.46) by replacing $H^{(0)}$ by $H^{(1)}$ and $H^{(2)}$ by $H^{(3)}$, respectively. The contribution of diagram (f) results from $V_{2\pi}^{\rm 5i}$ in Eq. (3.45) with $H^{(2)}$ being replaced by $H^{(3)}$ and has already been included in Eqs. (3.47). Finally, contributions of graphs (h), (i) and diagram (j) can be obtained by evaluating matrix elements of the operators $V_{2\pi}^{\rm 5e,5f}$ in Eq. (3.42) and $V_{2\pi}^{\rm 5g}$ in Eq. (3.43), respectively, where one of the vertices $H^{(0)}$ is replaced by the isospin-breaking πNN vertex $H^{(3)}$ from Eq. (2.6) and all possible permutations of the operators $H^{(3)}$ and $H^{(0)}$ are taken into account. Notice that in this case one only needs to keep the pionic free energy in the corresponding denominators. We found that diagrams (d), (g), and (j) lead to vanishing contributions while the subleading CSB potential generated by diagrams (c), (e), (h), and (i) in Fig. 6 reads

$$W_C^{(5)} = -\frac{1}{96\pi^2 F_\pi^4} L^\Lambda(q)\Big\{ -g_A^2\delta\bar{m}\frac{48M_\pi^4(2c_1+c_3)}{4M_\pi^2+q^2} + 4M_\pi^2\big[g_A^2\delta\bar{m}(18c_1+2c_2-3c_3) + (2\delta\bar{m}-(\delta\bar{m})^{\rm str}) \times(6c_1-c_2-3c_3)\big] + q^2\big[g_A^2\delta\bar{m}(5c_2-18c_3) - (2\delta\bar{m}-(\delta\bar{m})^{\rm str})(c_2+6c_3)\big]\Big\},$$
$$W_T^{(5)} = -\frac{1}{q^2}W_S^{(5)} = -\frac{g_A^2}{16\pi^2 F_\pi^4} L^\Lambda(q)\,(\delta\bar{m}c_4 + g_A\beta), \qquad (3.52)$$

where $\beta = \epsilon M_\pi^2(2d_{17}-d_{18}-2d_{19})$. Notice that we have also included the contribution of diagram (e) in Fig. 6 with the c_5-vertex being replaced by the f_2-vertex from Eqs. (2.6), which appears formally at order $\nu = 6$.[7] This contribution has precisely the same structure as the one proportional to the LEC c_5 with the overall strength $2(\delta\bar{m})^{\rm em}$ instead of $(\delta\bar{m})^{\rm str}$. In Eqs. (3.52) we have expressed $2(\delta\bar{m})^{\rm em} + (\delta\bar{m})^{\rm str}$ as $2\delta\bar{m} - (\delta\bar{m})^{\rm str}$.

To summarize, the charge-symmetry conserving 2PE potential is due to the pion mass difference and includes a central component at order $\nu = 4$ and tensor and spin-spin components at order $\nu = 5$ given in Eqs. (3.40) and (3.49), respectively. The CSB 2PE potential has all central, tensor and spin-spin components at orders $\nu = 4$ and $\nu = 5$, and the corresponding expressions are given in Eqs. (3.47) and (3.52). Further, we stress that our results for the isospin-violating 2PE potential are consistent with taking

$$g_A^2 = 4\pi\left(\frac{2F_\pi}{M_{\pi^\pm}}\right)^2 f_c^2 \qquad (3.53)$$

in the isospin-conserving 2PE potential. This expression already accounts for the Goldberger-Treiman discrepancy. Finally, to the order we are working, the constant β can be expressed in terms of the pion-nucleon coupling constants as follows:

$$\beta = \frac{f_p^2 - f_n^2}{8 f_c^2} g_A. \qquad (3.54)$$

C. Two-pion-exchange potential in coordinate space

Let us now take a look at the isospin-violating potential in coordinate space. Similar to Eq. (3.34) we define

$$V_{2\pi} = (\tau_1^3\tau_2^3)[\tilde{V}_C + \tilde{V}_S(\vec{\sigma}_1\cdot\vec{\sigma}_2) + \tilde{V}_T S_{12}] + (\tau_1^3+\tau_2^3)[\tilde{W}_C + \tilde{W}_S(\vec{\sigma}_1\cdot\vec{\sigma}_2) + \tilde{W}_T S_{12}], \qquad (3.55)$$

where $S_{12} = 3\vec{\sigma}_1\cdot\hat{r}\,\vec{\sigma}_2\cdot\hat{r} - \vec{\sigma}_1\cdot\vec{\sigma}_2$ and the functions $\tilde{V}_C(r), \ldots, \tilde{W}_T(r)$ depend on the distance r. Consider now the charge-symmetry-conserving 2PE potentials $\tilde{V}_i(r)$ which are due to the pion mass difference and correspond to $V_C^{(4)}$, $V_T^{(5)}$, and $V_S^{(5)}$ defined in Eqs. (3.40) and (3.49). In order to obtain the r-space expressions (at $r \neq 0$), one usually switches to the spectral-function representation for the nonpolynomial part of the potential which has the form

$$V_i(q) = \frac{2}{\pi}\int_{2M_\pi}^\infty d\mu\,\mu\frac{\text{Im}[V_i(-i\mu)]}{\mu^2+q^2}. \qquad (3.56)$$

Here, $\text{Im}[V_i(-i\mu)]$ is the mass spectrum (or the spectral function) entering this representation, which results from the analytical continuation of the momentum-space functions to $q = 0^+ - i\mu$. Using this representation one obtains for the

[7] The corresponding contribution $\propto f_1$ does not lead to isospin breaking and is not considered.

functions $\tilde{V}_i(r)$ for $r > 0$:

$$\tilde{V}_C(r) = \frac{1}{2\pi^2 r}\int_{2M_\pi}^{\infty} d\mu\, \mu e^{-\mu r}\mathrm{Im}[V_C(-i\mu)], \tag{3.57}$$

$$\tilde{V}_T(r) = -\frac{1}{6\pi^2 r^3}\int_{2M_\pi}^{\infty} d\mu\, \mu e^{-\mu r}(3+3\mu r+\mu^2 r^2) \times \mathrm{Im}[V_T(-i\mu)], \tag{3.58}$$

$$\tilde{V}_S(r) = -\frac{1}{6\pi^2 r}\int_{2M_\pi}^{\infty} d\mu\, \mu e^{-\mu r}(\mu^2\mathrm{Im}[V_T(-i\mu)] - 3\,\mathrm{Im}[V_S(-i\mu)]). \tag{3.59}$$

For the CSC 2PE potential $\propto \delta\bar{M}_\pi^2$ the spectral-function representation takes a slightly more complicated form as compared to Eq. (3.56), namely,

$$V_i(q) = \lim_{\epsilon\to 0}\left[\frac{2}{\pi}\int_{2M_\pi+\epsilon}^{\infty} d\mu\mu\frac{\mathrm{Im}[V_i(-i\mu)]}{\mu^2+q^2} - \frac{8M_\pi}{\pi}\frac{\mathrm{Im}[V_i(-2iM_\pi - i\epsilon)]}{4M_\pi^2+q^2}\right]. \tag{3.60}$$

The second term in this expression accounts for the corresponding shifts of the threshold when pions of different masses are exchanged between the nucleons. Notice that both terms in Eq. (3.60) go to infinity for $\epsilon \to 0$, but their sum is, of course, finite in this limit. Although one can, in principle, use this representation on order to obtain $\tilde{V}_i(r)$, we choose different strategy by using Eq. (3.38) in coordinate space. Substituting the expressions for the leading and subleading isospin-invariant 2PE potential in r-space [35,38] in Eq. (3.38), we find

$$\begin{aligned}
\tilde{V}_C^{(4)}(r)\Big|_{\Lambda\to\infty} &= \frac{\delta\bar{M}_\pi^2 M_\pi}{256\pi^3 F_\pi^4 r^2}\left[4g_A^2\left(-1+g_A^2\right)xK_0(2x) + \left(-1-6g_A^2+g_A^4(11+4x^2)\right)K_1(2x)\right],\\
\tilde{V}_T^{(5)}(r) &= \frac{\delta\bar{M}_\pi^2 g_A^2 c_4}{192\pi^2 F_\pi^4}\frac{e^{-2x}}{r^4}(4+x(5+2x)) - \frac{\delta\bar{M}_\pi^2 g_A^2 c_4}{384\pi^2 F_\pi^4}\frac{e^{-y}}{r^4}(8+y(5+y)),\\
\tilde{V}_S^{(5)}(r) &= -\frac{\delta\bar{M}_\pi^2 g_A^2 c_4}{96\pi^2 F_\pi^4}\frac{e^{-2x}}{r^4}(1+2x(1+x)) + \frac{\delta\bar{M}_\pi^2 g_A^2 c_4}{192\pi^2 F_\pi^4}\frac{e^{-y}}{r^4}(2+y(2+y)),
\end{aligned} \tag{3.61}$$

where $x = M_\pi r$, $y = \Lambda r$, and K_i are the modified Bessel functions. In the case of $\tilde{V}_C^{(4)}$, we could only perform the integral in Eq. (3.57) analytically for $\Lambda \to \infty$ which corresponds to the DR result. This expression can also be found in Ref. [6].

To obtain the CSB 2PE at orders $\nu = 4$ and $\nu = 5$ in r-space, it is convenient to use Eqs. (3.57)–(3.59) (with V_i being replaced by W_i). In that case, the spectral-function representation in Eq. (3.56) is valid. Using Eqs. (3.47) and (3.52) we find

$$\begin{aligned}
\tilde{W}_C^{(4)}(r) &= \frac{g_A^2}{256\pi^2 F_\pi^4}\frac{e^{-2x}}{r^4}\left((\delta\bar{m})^{\mathrm{str}}(1+x)^2 - 2\delta\bar{m}g_A^2(2+x(4+x(2+x)))\right) - \frac{g_A^2}{512\pi^2 F_\pi^4}\frac{e^{-y}}{r^4}\left((\delta\bar{m})^{\mathrm{str}} - 4\delta\bar{m}g_A^2\right)\times(2-2x^2+y(2+y)),\\
\tilde{W}_T^{(4)}(r) &= -\frac{\delta\bar{m}g_A^4}{384\pi^2 F_\pi^4}\frac{e^{-2x}}{r^4}(4+x(5+2x)) + \frac{\delta\bar{m}g_A^4}{768\pi^2 F_\pi^4}\frac{e^{-y}}{r^4}(8+y(5+y)),\\
\tilde{W}_S^{(4)}(r) &= \frac{\delta\bar{m}g_A^4}{192\pi^2 F_\pi^4}\frac{e^{-2x}}{r^4}(1+2x+2x^2) - \frac{\delta\bar{m}g_A^4}{384\pi^2 F_\pi^4}\frac{e^{-y}}{r^4}(2+2y+y^2),
\end{aligned} \tag{3.62}$$

and

$$\begin{aligned}
\tilde{W}_C^{(5)}(r)\Big|_{\Lambda\to\infty} &= \frac{M_\pi}{32\pi^3 F_\pi^4 r^4}\left[\left(g_A^2\delta\bar{m}x(-5c_2+18c_3 + 4(2c_1+c_3)x^2) + (2\delta\bar{m}-(\delta\bar{m})^{\mathrm{str}})\times x(c_2+6c_3)\right)K_0(2x) + \left(g_A^2\delta\bar{m}(-5c_2+18c_3 + 2(6c_1-c_2+5c_3)x^2) + (2\delta\bar{m}-(\delta\bar{m})^{\mathrm{str}})\times(c_2+6c_3+2(2c_1+c_3)x^2)\right)K_1(2x)\right],\\
\tilde{W}_T^{(5)}(r)\Big|_{\Lambda\to\infty} &= -\frac{g_A^2 M_\pi}{96\pi^3 F_\pi^4 r^4}(c_4\delta\bar{m}+\beta g_A)(12xK_0(2x) + (15+4x^2)K_1(2x)),\\
\tilde{W}_S^{(5)}(r)\Big|_{\Lambda\to\infty} &= \frac{g_A^2 M_\pi}{24\pi^3 F_\pi^4 r^4}(c_4\delta\bar{m}+\beta g_A)(3xK_0(2x) + (3+2x^2)K_1(2x)).
\end{aligned} \tag{3.63}$$

Expressions in Eq. (3.62) agree in the limit $\Lambda \to \infty$ with the ones given in Ref. [7]. Again, at order $\nu = 5$ we could only perform integrals in Eqs. (3.57)–(3.59) analytically for $\Lambda \to \infty$.

It is now interesting to compare the strength of the corresponding r-space potentials. Here and in what follows, we adopt the same values for the LECs c_i as in our work [27]: $c_1 = -0.81\ \mathrm{GeV}^{-1}$, $c_2 = 3.28\ \mathrm{GeV}^{-1}$, $c_3 = -3.40\ \mathrm{GeV}^{-1}$, and $c_4 = -3.40\ \mathrm{GeV}^{-1}$. Further, $g_A = 1.27$, $M_\pi = 138.03$ MeV, and $F_\pi = 92.4$ MeV. For the strong nucleon mass shift $(\delta m)^{\mathrm{str}}$, we use the value given in Eq. (3.14). Finally, in our numerical estimations we set $\beta = 0$ since the value of this LEC is not known at present. Notice, however, that a 1% relative deviation between f_p and f_n leads to $g_A\beta \sim \delta\bar{m}c_4$, so that the strength of the resulting CSB potential is comparable to the one of the CSB potential $\propto c_4$. The CSC and CSB 2PE

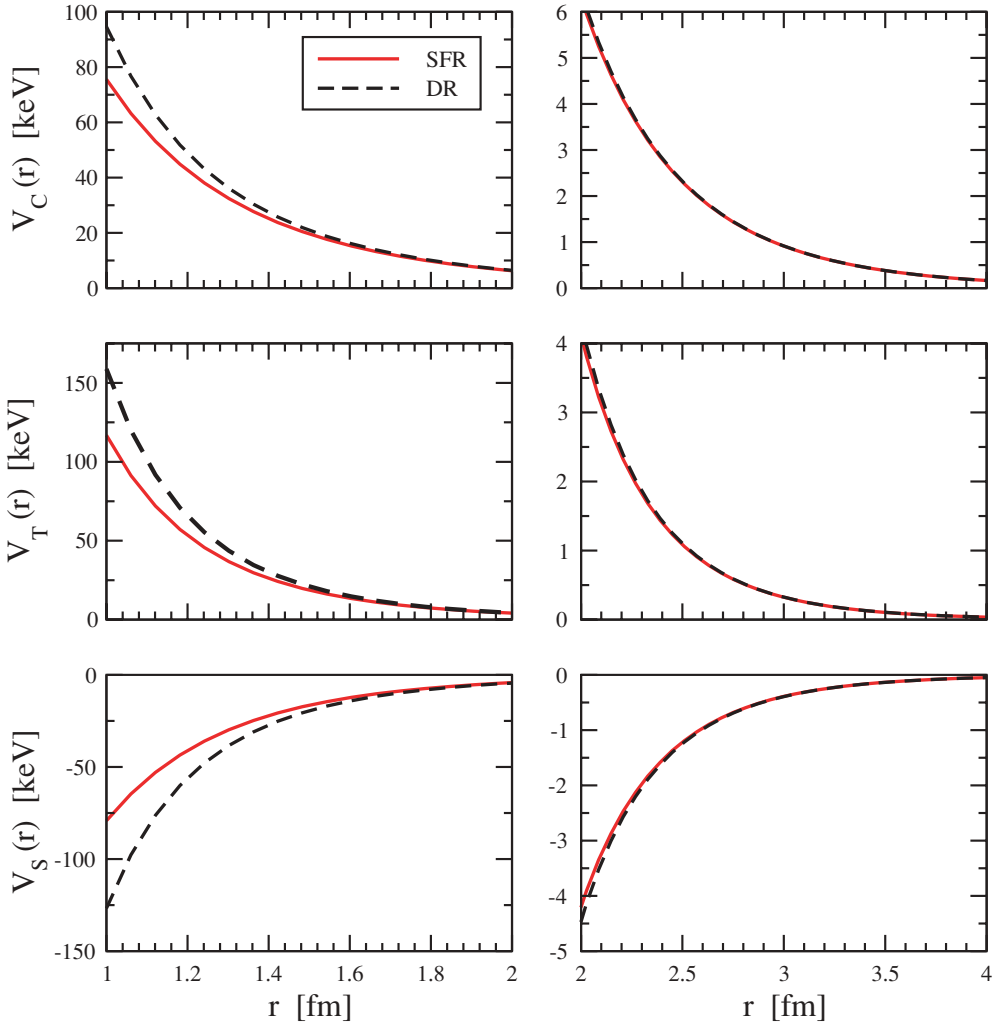

FIG. 7. (Color online) Central (upper row), tensor (middle row), and spin-spin (bottom row) components of the charge-symmetry-conserving (CSC) 2PE potential in coordinate space, utilizing DR (dashed) and SFR (solid lines). The SFR result corresponds to $\Lambda = 700$ MeV. Left/right panels: Distances from 1 . . . 2/2 . . . 4 fm.

potentials are plotted in Figs. 7 and 8, respectively, for two choices of the cut-off Λ in the SFR: $\Lambda = 700$ MeV and $\Lambda = \infty$ which is equivalent to DR. The results for $\tilde{V}_C^{(4)}(r)$ and $\tilde{W}_i^{(5)}(r)$ for $\Lambda = 700$ MeV are obtained numerically. First of all, we notice that all CSC 2PE contributions have similar strength $\sim$100 keV at $r = 1$ fm and $\sim 4 - 6$ keV at $r = 2$ fm. Although the central potential $V_C^{(4)}(r)$ is formally dominant, the subleading contributions $V_{T,S}^{(5)}(r)$ are numerically large due to the large value of the LEC c_4. To get further insights into the importance of the CSC 2PE potential, it is instructive to compare its strength with the strength of the corresponding 1PE potential resulting due to the pion mass difference, which provides the dominant isospin-violating contribution to the NN force at order $\nu = 2$. It has the following form in momentum space:

$$V_T^{(2)}(q) = -\left(\frac{g_A}{2F_\pi}\right)^2 \delta\bar{M}_\pi^2 \frac{(\vec{\sigma}_1 \cdot \vec{q}\,)(\vec{\sigma}_2 \cdot \vec{q}\,)}{\left(q^2 + M_\pi^2\right)^2}. \quad (3.64)$$

The corresponding r-space expressions read (for $r > 0$)

$$\begin{aligned} \tilde{V}_T^{(2)}(r) &= \frac{g_A^2 \delta\bar{M}_\pi^2}{96\pi F_\pi^2} \frac{e^{-x}}{r}(1+x), \\ \tilde{V}_S^{(2)}(r) &= -\frac{g_A^2 \delta\bar{M}_\pi^2}{96\pi F_\pi^2} \frac{e^{-x}}{r}(2-x). \end{aligned} \quad (3.65)$$

In Fig. 9 we have plotted the ratio $\tilde{V}_T^{(5)}/\tilde{V}_T^{(2)}$ as a function of r. The 2PE contribution is significant for $r \lesssim 2$ fm. At larger distances it becomes negligible (less than 1% for $r \gtrsim 3.5$ fm) compared to the 1PE contribution due to its shorter range.

Let us now switch to the CSB contributions displayed in Fig. 8. Similar to the CSC potential, the subleading terms $\propto c_i$ are numerically enhanced due to large values of these LECs. The strongest contribution is given by the subleading central potential which reaches $\sim 150 - 300$ keV at $r = 1$ fm and $\sim$6 keV at $r = 2$ fm and is dominated by terms $\propto c_3$. This is similar to the isospin-symmetric case, where the subleading central 2PE potential is known to be very strong.

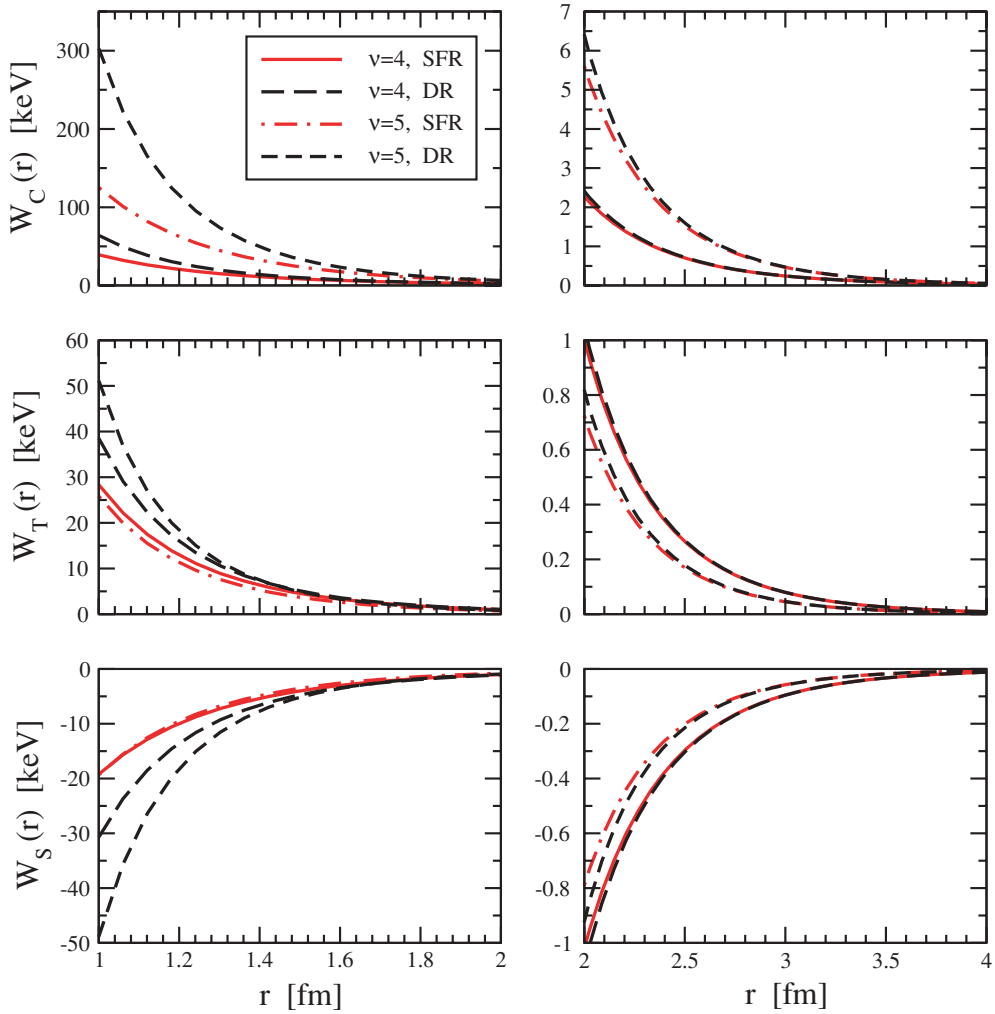

FIG. 8. (Color online) Central (upper row), tensor (middle row), and spin-spin (bottom row) components of the charge-symmetry-breaking 2PE potential in coordinate space. Long-/short-dashed lines: DR at $\nu = 4$ and $\nu = 5$; Solid/dot-dashed lines: SFR at $\nu = 4$ and $\nu = 5$. The SFR results correspond to $\Lambda = 700$ MeV.

To enable a more detailed comparison between the leading and subleading contributions to the CSB 2PE potential, we plot in Fig. 10 the corresponding ratios. While the subleading central component is significantly stronger than the leading one in a wide range of distances r, the tensor and spin-spin components are of the same size as the leading ones only for $r \lesssim 2$ fm. One should, however, keep in mind that our results obtained within the heavy baryon formalism using the leading-order approximation for the nucleon propagator become formally invalid at very large distances. This problem with the heavy baryon formalism has been first observed in the single-nucleon sector and can be dealt with using, e.g., the Lorentz invariant

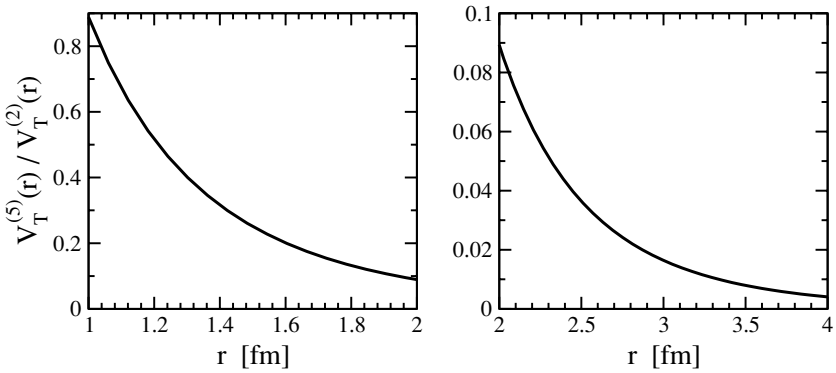

FIG. 9. Ratio of the CSC tensor 2π-exchange (using SFR with $\Lambda = 700$ MeV) and 1π-exchange potentials as a function of r.

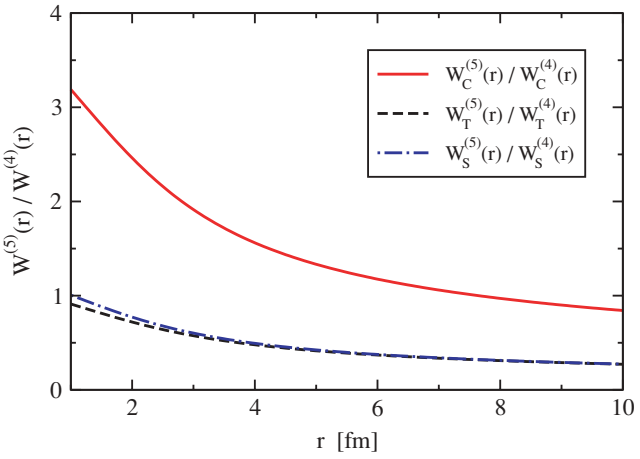

FIG. 10. (Color online) Ratio of the subleading ($\nu = 5$) and leading ($\nu = 4$) CSB 2PE potential as a function of r. Solid/dashed/dot-dashed line: central/tensor/spin-spin component. All results correspond to SFR with $\Lambda = 700$ MeV.

scheme proposed by Becher and Leutwyler [39], see also Ref. [40]. It is clear, however, that the NN interaction due to two-pion exchange becomes very weak at large distances, so that the problem with the formal inconsistency of the heavy baryon approach is expected to have little relevance for practical applications, see Ref. [41] for more details.

Finally, we would like to emphasize that the SFR results for CSC and the leading CSB contributions are rather close to the ones obtained in DR even for 1 fm $< r <$ 1.5 fm, see Fig. 7. Stated differently, the corresponding potentials seem to be strongly dominated by long-range components in 2π-exchange. Deviations between the SFR and DR results at short distances are significantly larger for CSB contributions at order $\nu = 5$. This is consistent with the fact that new CSB short-range terms with two derivatives start to contribute at this order. One expects that such new counterterms will largely remove the dependence of observables on the cutoff in the spectral-function representation.

D. Contact terms

We now discuss short-range isospin-breaking interactions. The leading contact terms in the NN potential at $\nu = 3$ are proportional to the quark mass difference and violate charge symmetry [1,2,5,7]:

$$V_{\rm cont}^{(3)} = \beta_{3,1}\left(\tau_1^3 + \tau_2^3\right) + \beta_{3,2}\,\vec{\sigma}_1 \cdot \vec{\sigma}_2\left(\tau_1^3 + \tau_2^3\right), \quad (3.66)$$

where $\beta_{3,i} \sim \epsilon M_\pi^2/(F_\pi^2\Lambda^2)$ are constants. We remind the reader that the subscripts of the spin and isospin matrices refer to nucleon labels while the superscripts denote the corresponding vector indices. Both terms in Eq. (3.66) lead to the same structure in the potential when antisymmetrization with respect to the nucleons is performed. Consequently, it is sufficient to keep only one term.[8] At order $\nu = 4$ one has to take into account isospin-violating short-range interactions without derivatives of electromagnetic origin. In addition to the terms which have the same structure as the ones in Eq. (3.66) and thus only provide order $\sim e^2/(4\pi F_\pi)^2$ shifts of $\beta_{3,i}$, new CSC interactions appear:

$$V_{\rm cont}^{(4)} = \beta_{4,1}\tau_1^3\tau_2^3 + \beta_{4,2}\,\vec{\sigma}_1 \cdot \vec{\sigma}_2\tau_1^3\tau_2^3. \quad (3.67)$$

Again, one of these two terms can be eliminated performing antisymmetrization of the potential. Finally, at order $\nu = 5$ one needs to include CSB terms with two derivatives which are proportional to the quark mass difference. In the two-nucleon c.m. these terms read

$$\begin{aligned} V_{\rm cont}^{(5)} &= \left(\tau_1^3 + \tau_2^3\right)\Big[\beta_{5,1}\vec{q}^{\,2} + \beta_{5,2}\vec{k}^2 + (\beta_{5,3}\vec{q}^{\,2} + \beta_{5,4}\vec{k}^2)(\vec{\sigma}_1 \cdot \vec{\sigma}_2) \\ &\quad + \frac{i}{2}\beta_{5,5}(\vec{\sigma}_1 + \vec{\sigma}_2) \cdot (\vec{k} \times \vec{q}) + \beta_{5,6}\,(\vec{\sigma}_1 \cdot \vec{q})(\vec{\sigma}_2 \cdot \vec{q}) \\ &\quad + \beta_{5,7}\,(\vec{\sigma}_1 \cdot \vec{k})(\vec{\sigma}_2 \cdot \vec{k})\Big] + i\beta_{5,8}\left(\tau_1^3 - \tau_2^3\right)\vec{k} \times \vec{q} \cdot (\vec{\sigma}_1 - \vec{\sigma}_2) \\ &\quad + i\beta_{5,9}[\boldsymbol{\tau}_1 \times \boldsymbol{\tau}_2]^3\vec{k} \times \vec{q} \cdot [\vec{\sigma}_1 \times \vec{\sigma}_2] + i\beta_{5,10}[\boldsymbol{\tau}_1 \times \boldsymbol{\tau}_2]^3 \\ &\quad \times ((\vec{\sigma}_1 \cdot \vec{q})(\vec{\sigma}_2 \cdot \vec{k}) - (\vec{\sigma}_1 \cdot \vec{k})(\vec{\sigma}_2 \cdot \vec{q})), \end{aligned} \quad (3.68)$$

where $\beta_{5,i} \sim \epsilon M_\pi^2/(F_\pi^2\Lambda^4)$ are further constants and $\vec{k} = (\vec{p} + \vec{p}\,')/2$. Performing antisymmetrization of this potential, it is easy to see that half of the terms proportional to $\beta_{5,1}, \beta_{5,2}, \beta_{5,3}, \beta_{5,4}, \beta_{5,6}$, and $\beta_{5,7}$ are redundant. Similarly, terms proportional to $\beta_{5,8}, \beta_{5,9}$, and $\beta_{5,10}$, which lead to mixing between the $T = 1$ and $T = 0$ states, generate the same structure when the potential is antisymmetrized. We are, therefore, left with five independent short-range terms at order $\nu = 5$ (for example, one can take terms proportional to $\beta_{5,1}, \beta_{5,3}, \beta_{5,5}, \beta_{5,6}$, and $\beta_{5,8}$).

The isospin-breaking short-range terms up to order $\nu = 5$ feed into the matrix-elements of the S- and P-waves in the following way:

$$\begin{aligned} \langle {}^1S_0,\ pp|V_{\rm cont}|{}^1S_0,\ pp\rangle &= \tilde{\beta}_{1S0}^{pp} + \beta_{1S0}(p^2 + p'^2), \\ \langle {}^1S_0, nn|V_{\rm cont}|{}^1S_0, nn\rangle &= \tilde{\beta}_{1S0}^{nn} - \beta_{1S0}(p^2 + p'^2), \\ \langle {}^3P_0,\ pp|V_{\rm cont}|{}^3P_0,\ pp\rangle &= -\langle {}^3P_0,\ nn|V_{\rm cont}|{}^3P_0,\ nn\rangle \\ &= \beta_{3P0}\,pp', \\ \langle {}^3P_1,\ pp|V_{\rm cont}|{}^3P_1,\ pp\rangle &= -\langle {}^3P_1,\ nn|V_{\rm cont}|{}^3P_1,\ nn\rangle \\ &= \beta_{3P1}\,pp', \\ \langle {}^3P_2,\ pp|V_{\rm cont}|{}^3P_2,\ pp\rangle &= -\langle {}^3P_2,\ nn|V_{\rm cont}|{}^3P_2,\ nn\rangle \\ &= \beta_{3P2}\,pp', \\ \langle {}^1P_1, np|V_{\rm cont}|{}^3P_1, np\rangle &= \beta_{1P1-3P1}\,pp', \end{aligned} \quad (3.69)$$

where the new LECs $\tilde{\beta}_{1S0}^{pp}$, $\tilde{\beta}_{1S0}^{nn}$, β_{1S0}, β_{3P0}, β_{3P1}, and $\beta_{1P1-3P1}$ can be expressed in terms of linear combinations of the LECs $\beta_{3,i}$, $\beta_{4,i}$, and $\beta_{5,i}$. Notice that we have adopted here the convention according to which the np matrix elements [with exception of the last term in Eq. (3.69)] do not change by switching off isospin-violating contact terms.

As pointed out in Ref. [5], one should, in principle, also take into account isospin-violating CSC contact terms associated with the contributions to the 2PE potential $\propto M_\pi^2$. These terms arise since the derivative in Eq. (3.38) has to be applied

[8] Equivalently, one can apply a Fierz transformation in the corresponding Lagrangian in order to eliminate redundant terms.

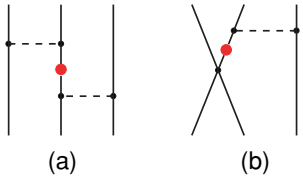

FIG. 11. (Color online) Isospin violating 3NF diagrams which include reducible topologies. For notation, see Figs. 1 and 2.

not only to the nonpolynomial part of $V^1_{2\pi}(M_\pi)$, but also to the corresponding counterterms which depend on M_π. The resulting CSC contact terms have fixed coefficients (in terms of g_A and F_π) and are of the order $\sim\delta\bar{M}_\pi^2/M_\pi^2$ instead of expected $\sim\delta\bar{M}_\pi^2/\Lambda^2$ compared to the corresponding isospin-invariant terms. We have found that these contact interactions cancel against the ones which result from taking the derivative of the nonpolynomial part of $V^1_{2\pi}(M_\pi)$. Thus, Eqs. (3.40) and (3.49) give the complete result for the corresponding CSC 2PE potential, and no additional contact terms need to be taken into account. Finally, we stress that no contact interactions depending on the total two-nucleon momentum $\vec{P}$ [similar to Eqs. (3.27) and (3.28)] appear up to the order $\nu = 5$.

IV. CONSISTENCY OF THE 2*N* AND 3*N* FORCES

It is well known that two- and three-nucleon forces have to be consistent with each other. In Refs. [9] and [42] we have derived isospin-violating 3NF at orders $\nu = 4$ and $\nu = 5$.[9] It has 1PE, 2PE and contact pieces and results from insertions of pion and nucleon mass differences as well as the c_5- and $f_{1,2}$-vertices in Eq. (2.6). Two 3NF diagrams out of seven shown in Fig. 1 of Ref. [42] appear to be of a special interest due to the fact that they include reducible topologies, i.e., time-ordered graphs with purely nucleonic intermediate states. These two diagrams are depicted in Fig. 11 and lead to the following contributions to the 3NF at order $\nu = 4$:

$$
\begin{aligned}
V^{11a} &= \sum_{i\neq j\neq k} 2\delta\bar{m}\left(\frac{g_A}{2F_\pi}\right)^4 \frac{(\vec{\sigma}_i\cdot\vec{q}_i)(\vec{\sigma}_j\cdot\vec{q}_j)}{\left(\vec{q}_i{}^2+M_\pi^2\right)^2\left(\vec{q}_j{}^2+M_\pi^2\right)} \\
&\quad\times\Big\{[\vec{q}_i\times\vec{q}_j]\cdot\vec{\sigma}_k[\boldsymbol{\tau}_i\times\boldsymbol{\tau}_j]^3 \\
&\qquad+\vec{q}_i\cdot\vec{q}_j\big[(\boldsymbol{\tau}_i\cdot\boldsymbol{\tau}_k)\tau_j^3-(\boldsymbol{\tau}_i\cdot\boldsymbol{\tau}_j)\tau_k^3\big]\Big\}, \\
V^{11b} &= \sum_{i\neq j\neq k} 2\delta\bar{m}C_T\left(\frac{g_A}{2F_\pi}\right)^2 \\
&\quad\times\frac{\vec{\sigma}_i\cdot\vec{q}_i}{\left(\vec{q}_i{}^2+M_\pi^2\right)^2}[\boldsymbol{\tau}_k\times\boldsymbol{\tau}_i]^3\,[\vec{\sigma}_j\times\vec{\sigma}_k]\cdot\vec{q}_i,
\end{aligned}
\tag{4.1}
$$

[9] Some of the charge-symmetry breaking 3NF contributions at order $\nu = 4$ were also considered in Ref. [43].

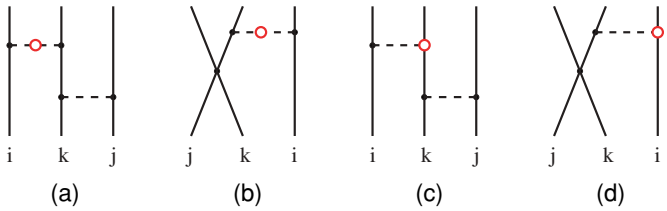

FIG. 12. (Color online) Feynman diagrams contributing to the CSB 3*N* scattering amplitude. Graphs resulting from the interchange of the nucleon lines and/or application of the time reversal operation are not shown. Empty circles denote insertions of the $\delta\bar{m}$-vertices from Eq. (4.2).

where i, j, and k are nucleon labels and $\vec{q}_i = \vec{p}\,'_i - \vec{p}_i$. Further, C_T is one of the two leading order four-nucleon LECs [16]. Notice that these nonvanishing contributions are in strong contrast to the corresponding isospin-invariant 3NF forces $\propto g_A^4$ and $\propto g_A^2 C_i$ as well as isospin-breaking ones $\propto \delta\bar{M}_\pi^2 g_A^4$ and $\propto \delta\bar{M}_\pi^2 g_A^2 C_i$ which are known to vanish, see, e.g., Refs. [44–46]. We also emphasize that these 3NF contributions were not explicitly evaluated in Ref. [43]. It is, therefore, important to look at the origin of these particular 3NFs in more detail. To that aim we evaluate the 3*N* scattering amplitude $\propto \delta\bar{m}g_A^4$ and $\propto \delta\bar{m}g_A^2 C_T$ and compare the result with the iterated 2*N* potential. We will demonstrate that the iterated 2NF + 3NF given in Eq. (4.1) reproduces correctly the 3*N* scattering amplitude. This is an excellent and rather nontrivial check of our results.

The most convenient way to evaluate the scattering amplitude is using the Feynman graph technique. In the following, we will use the method suggested in Ref. [8], in which the proton-to-neutron mass difference is removed from the Lagrangian by an appropriate field redefinition in favor of new isospin-violating terms $\propto \delta\bar{m}$ which are easier to handle in practical applications. Only two of such new isospin-breaking terms may lead to contributions $\propto \delta\bar{m}g_A^4$ and $\propto \delta\bar{m}g_A^2 C_T$ in the amplitude:

$$
\mathcal{L}' = \delta\bar{m}(\boldsymbol{\pi}\times\dot{\boldsymbol{\pi}})_3 - \frac{g_A}{4F_\pi}\frac{\delta\bar{m}}{m}N^\dagger\{\vec{\sigma}\cdot\vec{p},\ (\boldsymbol{\tau}\times\boldsymbol{\pi})_3\}N. \tag{4.2}
$$

Notice that in contrast to nuclear forces, the on-shell scattering amplitude we are interested in is unique and does not depend on field redefinitions. The relevant Feynman diagrams are shown in Fig. 12. Notice that Feynman graphs resulting from diagrams (a) and (b) with one of the g_A-vertices being replaced by the vertex corresponding to the second term in Eq. (2.5) lead to contributions $\propto 1/m$ which are irrelevant for our discussion. The contribution from graph (a) is given by

$$
\begin{aligned}
T^{12a} &= i\left(\frac{g_A}{2F_\pi}\right)^4 \frac{i^2}{\left[q_i{}^2-M_\pi^2+i\epsilon\right]^2}\,\frac{i2m\Lambda_+}{\left[\tilde{p}_k{}^2-m^2+i\epsilon\right]} \\
&\quad\times\frac{i}{\left[q_j{}^2-M_\pi^2+i\epsilon\right]}(\vec{\sigma}_i\cdot\vec{q}_i)(-\vec{\sigma}_k\cdot\vec{q}_i)(\vec{\sigma}_k\cdot\vec{q}_j) \\
&\quad\times(-\vec{\sigma}_j\cdot\vec{q}_j)(-2\delta\bar{m})(q_i)_0\epsilon_{ab3}\tau_i^b\tau_k^a(\boldsymbol{\tau}_k\cdot\boldsymbol{\tau}_j),
\end{aligned}
\tag{4.3}
$$

where we use the relativistic nucleon propagator. Here, Λ_+ is the projection matrix onto positive-energy states and

$\tilde{p}_k = p_k' + q_i = p_k' + p_i' - p_i = (\sqrt{\vec{p}_k'^{\,2} + m^2} + \sqrt{\vec{p}_i'^{\,2} + m^2} - \sqrt{\vec{p}_i^{\,2} + m^2},\ \vec{p}_k' + \vec{q}_i)$ is the four-momentum of the nucleon k in the intermediate state. Notice further that the amplitude is multiplied by i in order to match with the standard normalization of the nonrelativistic T-matrix. The consistency of this procedure can be verified, e.g., by calculating the static isospin-invariant 1PE potential. Using the relation

$$\frac{i2m\Lambda_+}{\left[\tilde{p}_k{}^2 - m^2 + i\epsilon\right]} = \frac{i}{\delta T + i\epsilon} + \mathcal{O}\left(\frac{1}{m}\right), \tag{4.4}$$

where $\delta T = (\vec{p}_i{}'^2 + \vec{p}_k{}'^2 - \vec{p}_i{}^2 - \vec{\tilde{p}}_k{}^2)/2m$, we can express T^{12a} as (modulo $1/m^2$-corrections):

$$T^{12a} = -i2\delta\bar{m} v_{ik}^2 [\boldsymbol{\tau}_i \times \boldsymbol{\tau}_k]^3 \left(\frac{\vec{p}_i{}'^2}{2m} - \frac{\vec{p}_i{}^2}{2m}\right) \frac{1}{\delta T + i\epsilon} v_{kj}^1 (\boldsymbol{\tau}_k \cdot \boldsymbol{\tau}_j), \tag{4.5}$$

where

$$v_{ik}^n = -\left(\frac{g_A}{2F_\pi}\right)^2 \frac{(\vec{\sigma}_i \cdot \vec{q}_i)(\vec{\sigma}_k \cdot \vec{q}_i)}{\left(\vec{q}_i{}^2 + M_\pi^2\right)^n}. \tag{4.6}$$

We now use the equality

$$\left(\frac{\vec{p}_i{}'^2}{2m} - \frac{\vec{p}_i{}^2}{2m}\right) = \frac{1}{2}\left(\frac{\vec{p}_i{}'^2}{2m} - \frac{\vec{p}_i{}^2}{2m} - \frac{\vec{p}_k{}'^2}{2m} + \frac{\vec{\tilde{p}}_k{}^2}{2m} + \delta T\right), \tag{4.7}$$

to rewrite Eq. (4.5) in the form

$$T^{12a} = i\frac{\delta\bar{m}}{2m} v_{ik}^2 [\boldsymbol{\tau}_i \times \boldsymbol{\tau}_k]^3 \left(\vec{p}_i{}^2 - \vec{\tilde{p}}_k{}^2 - \vec{p}_i{}'^2 + \vec{p}_k{}'^2\right) \times \frac{1}{\delta T + i\epsilon} v_{kj}^1 (\boldsymbol{\tau}_k \cdot \boldsymbol{\tau}_j) - i\delta\bar{m} v_{ik}^2 [\boldsymbol{\tau}_i \times \boldsymbol{\tau}_k]^3 v_{kj}^1 (\boldsymbol{\tau}_k \cdot \boldsymbol{\tau}_j). \tag{4.8}$$

The first term in the above equation can be identified with the iteration of the isospin-violating 1PE potential in Eq. (3.28) between the nucleons i and k and the isospin-invariant static 1PE potential between the nucleons k and j, $V_{1\pi} = v_{kj}^1 (\boldsymbol{\tau}_k \cdot \boldsymbol{\tau}_j)$. The second term in Eq. (4.8) thus corresponds to the genuine contribution of the 3NF. Performing the algebra for spin and isospin matrices, we obtain the following result:

$$\begin{aligned} &-i\delta\bar{m} v_{ik}^2 [\boldsymbol{\tau}_i \times \boldsymbol{\tau}_k]^3 v_{kj}^1 (\boldsymbol{\tau}_k \cdot \boldsymbol{\tau}_j) \\ &= \delta\bar{m} \left(\frac{g_A}{2F_\pi}\right)^4 \frac{(\vec{\sigma}_i \cdot \vec{q}_i)(\vec{\sigma}_j \cdot \vec{q}_j)}{\left(\vec{q}_i{}^2 + M_\pi^2\right)^2 \left(\vec{q}_j{}^2 + M_\pi^2\right)} \\ &\quad \times \Big\{ [\vec{q}_i \times \vec{q}_j] \cdot \vec{\sigma}_k [\boldsymbol{\tau}_i \times \boldsymbol{\tau}_j]^3 + \vec{q}_i \cdot \vec{q}_j \big[(\boldsymbol{\tau}_i \cdot \boldsymbol{\tau}_k)\tau_j^3 \\ &\quad - (\boldsymbol{\tau}_i \cdot \boldsymbol{\tau}_j)\tau_k^3\big] - i\vec{q}_i \cdot \vec{q}_j [\boldsymbol{\tau}_i \times \boldsymbol{\tau}_j]^3 + i[\vec{q}_i \times \vec{q}_j] \\ &\quad \times \vec{\sigma}_k \big[(\boldsymbol{\tau}_i \cdot \boldsymbol{\tau}_k)\tau_j^3 - (\boldsymbol{\tau}_i \cdot \boldsymbol{\tau}_j)\tau_k^3\big] \Big\}. \end{aligned} \tag{4.9}$$

To get the complete expression for the 3NF we need to take into account the contribution of the diagram resulting from graph (a) in Fig. 12 by interchanging the ordering of the pion propagators and summing over the nucleon labels. This leads to cancellation of the terms in the third line of Eq. (4.9). The final result agrees with V^{11a} in Eq. (4.1).

Similarly, the scattering amplitude corresponding to the graph (b) in Fig. 12 is

$$T^{12b} = -i2\delta\bar{m} v_{ik}^2 [\boldsymbol{\tau}_i \times \boldsymbol{\tau}_k]^3 \left(\frac{\vec{p}_i{}'^2}{2m} - \frac{\vec{p}_i{}^2}{2m}\right) \times \frac{1}{\delta T + i\epsilon} [C_S + C_T (\vec{\sigma}_j \cdot \vec{\sigma}_k)]. \tag{4.10}$$

Notice that we use the following Feynman rule for contact terms: $(-i)[C_S + C_T(\vec{\sigma}_j \cdot \vec{\sigma}_k]$, which leads to the $2N$ potential $V = C_S + C_T(\vec{\sigma}_j \cdot \vec{\sigma}_k)$. We rewrite the amplitude T^{12b} in the form

$$\begin{aligned} T^{12b} &= i\frac{\delta\bar{m}}{2m} v_{ik}^2 [\boldsymbol{\tau}_i \times \boldsymbol{\tau}_k]^3 \left(\vec{p}_i{}^2 - \vec{\tilde{p}}_k{}^2 - \vec{p}_i{}'^2 + \vec{p}_k{}'^2\right) \\ &\quad \times \frac{1}{\delta T + i\epsilon} [C_S + C_T (\vec{\sigma}_j \cdot \vec{\sigma}_k)] \\ &\quad - i\delta\bar{m} v_{ik}^2 [\boldsymbol{\tau}_i \times \boldsymbol{\tau}_k]^3 [C_S + C_T (\vec{\sigma}_j \cdot \vec{\sigma}_k)]. \end{aligned} \tag{4.11}$$

Again, the term in the first line of the above equation gives the iterative contribution to the amplitude, while the term in the second line is the genuine 3NF contribution:

$$\begin{aligned} &-i\delta\bar{m} v_{ik}^2 [\boldsymbol{\tau}_i \times \boldsymbol{\tau}_k]^3 [C_S + C_T (\vec{\sigma}_j \cdot \vec{\sigma}_k)] \\ &= \delta\bar{m} \left(\frac{g_A}{2F_\pi}\right)^2 \frac{\vec{\sigma}_i \cdot \vec{q}_i}{\left(\vec{q}_i{}^2 + M_\pi^2\right)^2} [\boldsymbol{\tau}_i \times \boldsymbol{\tau}_k]^3 \{ iC_S (\vec{\sigma}_k \cdot \vec{q}_i) \\ &\quad + iC_T (\vec{\sigma}_j \cdot \vec{q}_i) - C_T [\vec{\sigma}_j \times \vec{\sigma}_k] \cdot \vec{q}_i \}. \end{aligned} \tag{4.12}$$

The first two terms in the curly brackets cancel against the contribution of the time-reversed diagram, so that the final result agrees with V^{11b} in Eq. (4.1).

Finally, it is easy to see that the amplitude corresponding to graphs (c) and (d) in Fig. 12 is reproduced by the iteration of the isospin-breaking 1PE potential in Eq. (3.27) and the leading isospin-symmetric $2N$ potential with no need for an additional 3NF. We thus have verified the consistency of our results for isospin-violating 1PE $2N$ force and 3NFs.

V. SUMMARY AND OUTLOOK

The pertinent findings of this study can be summarized as follows:

(i) We have applied the method of unitary transformation to study the isospin-breaking NN forces. We have derived *all* forces (in the absence of virtual photons) up to $\nu = 5$ in the chiral expansion. Together with the 3NFs worked out in Ref. [9], this completely specifies the isospin-breaking few-nucleon forces up to this order.

(ii) The isospin-violating one-pion exchange potential is a combination of terms of order $\nu = 2, 3, 4$, and 5. It is specified in Eqs. (3.19), (3.27), (3.28), and (3.30). In particular, we have reproduced the expressions for the 1PE potential, class IV, found recently in Ref. [8].

(iii) The results for the isospin-violating 2PE potential in momentum space are given in Eqs. (3.40), (3.47), (3.49), and (3.52). The corresponding expressions in coordinate space are discussed in detail in Sec. III C. In particular, we have reproduced the expressions for the 2PE potential

at order $\nu = 4$ worked out in Refs. [7,36]. The main new result is the 2PE potential at order $\nu = 5$ which has not been considered in EFT before. We find that the derived subleading CSB 2PE at order $\nu = 5$ gives numerically the *dominant* contribution to the CSB TPE potential, cf. Figs. 8, and 10. As in the isospin-conserving case, this effect can be traced back to the large magnitude of the dimension two pion-nucleon LECs c_2, c_3, and c_4 (which is well understood, see Ref. [47]).

(iv) The contact interactions appear at orders $\nu = 3, 4, 5$ and are listed in Eq. (3.69). These are parametrized in terms of the LECs $\tilde{\beta}_i$ and β_i.

(v) We have also demonstrated explicitely that our results for the isospin-violating 2*N* and 3*N* forces are consistent with each other.

These results pave the way for new precision studies. To make this point more transparent, we reiterate that the finite-range part of the potential, i.e., the 1PE and 2PE pieces, depend on the mass shifts $\delta\bar{M}_\pi^2$ and $\delta\bar{m}$ which are well known, and the strong nucleon mass shift $(\delta\bar{m})^{\rm str}$ which is less well known. For the latter quantity, one can use the value based on the Cottingham sum rule, see Eq. (3.14). In addition, the pion-nucleon coupling constants f_p^2, f_n^2, and f_c^2 are not well known at present. In principle, these constants can be extracted from an independent partial wave analysis of the *pp* and *np* data, such as the new Nijmegen PWA [48]. Provided such an extraction is possible, the finite-range part of the isospin-violating nucleon force is completely determined. One can then try to fix the values of the LECs $\tilde{\beta}_i$ and β_i from the low partial waves in the *np* and *pp* systems in order to make predictions for the corresponding *nn* partial waves. It remains to be seen whether this ambitious program can be carried out. Also, one should keep in mind that the isospin-conserving *NN* forces have so far only been worked out up to order $\nu = 4$ in the power counting.

ACKNOWLEDGMENTS

E. E. would like to thank Prof. W. Glöckle for helpful discussions and warm hospitality during his stay in Bochum, where part of this work has been done. This work has been supported by the U.S. Department of Energy Contract No. DE-AC05-84ER40150 under which the Southeastern Universities Research Association (SURA) operates the Thomas Jefferson National Accelerator Facility and by the Deutsche Forschungsgemeinschaft through funds provided to the SFB/TR 16 "Subnuclear Structure of Matter." This research is part of the EU Integrated Infrastructure Initiative Hadron Physics Project under Contract No. RII3-CT-2004-506078.

[1] U. L. van Kolck, "Soft physics: Applications of effective chiral lagrangians to nuclear physics and quark models," Ph.D. thesis, University of Texas, Austin, USA, 1993, UMI-94-01021.
[2] U. van Kolck, J. L. Friar, and T. Goldman, Phys. Lett. **B371**, 169 (1996).
[3] U. van Kolck, M. C. M. Rentmeester, J. L. Friar, T. Goldman, and J. J. de Swart, Phys. Rev. Lett. **80**, 4386 (1998).
[4] E. Epelbaum and U.-G. Meißner, Phys. Lett. **B461**, 287 (1999).
[5] M. Walzl, U.-G. Meißner, and E. Epelbaum, Nucl. Phys. **A693**, 663 (2001).
[6] J. L. Friar and U. van Kolck, Phys. Rev. C **60**, 034006 (1999).
[7] J. L. Friar, U. van Kolck, G. L. Payne, and S. A. Coon, Phys. Rev. C **68**, 024003 (2003).
[8] J. L. Friar, U. van Kolck, M. C. M. Rentmeester, and R. G. E. Timmermans, Phys. Rev. C **70**, 044001 (2004).
[9] E. Epelbaum, U.-G. Meißner, and J. E. Palomar, Phys. Rev. C **71**, 024001 (2005).
[10] H. Leutwyler, Phys. Lett. **B374**, 163 (1996).
[11] R. Urech, Nucl. Phys. **B433**, 234 (1995).
[12] U.-G. Meißner and S. Steininger, Phys. Lett. **B419**, 403 (1998).
[13] G. Müller and U.-G. Meißner, Nucl. Phys. **B556**, 265 (1999).
[14] U. van Kolck, Few Body Syst. Suppl. **9**, 444 (1995).
[15] S. Weinberg, Phys. Lett. **B251**, 288 (1990).
[16] S. Weinberg, Nucl. Phys. **B363**, 3 (1991).
[17] V. Bernard, N. Kaiser, and U.-G. Meißner, Int. J. Mod. Phys. E **4**, 193 (1995).
[18] N. Fettes and U.-G. Meißner, Nucl. Phys. **A693**, 693 (2001).
[19] E. Epelbaum, U.-G. Meißner, and W. Glöckle, Nucl. Phys. **A714**, 535 (2003).
[20] S. Steininger, "Reelle und virtuelle photonen in chiraler Störungstheorie," Ph.D. thesis, University Bonn, Germany, 1999.
[21] N. Fettes, U.-G. Meißner, M. Mojzis, and S. Steininger, Ann. Phys. (NY) **283**, 273 (2000).
[22] J. Gasser, M. A. Ivanov, E. Lipartia, M. Mojzis, and A. Rusetsky, Eur. Phys. J. C **26**, 13 (2002).
[23] E. A. Ueling, Phys. Rev. **48**, 55 (1935).
[24] L. Durand III, Phys. Rev. **108**, 1597 (1957).
[25] G. J. M. Austen and J. J. de Swart, Phys. Rev. Lett. **50**, 2039 (1983).
[26] V. G. J. Stoks and J. J. de Swart, Phys. Rev. C **42**, 1235 (1990).
[27] E. Epelbaum, W. Glöckle, and U.-G. Meißner, Nucl. Phys. **A747**, 362 (2005).
[28] E. Epelbaum, W. Glöckle, and U.-G. Meißner, Nucl. Phys. **A637**, 107 (1998).
[29] S. Okubo, Prog. Theor. Phys. (Jpn) **12**, 603 (1954).
[30] G. Ecker and M. Mojzis, Phys. Lett. **B410**, 266 (1997).
[31] S. Steininger, U.-G. Meißner, and N. Fettes, J. High Energy Phys. 09 (1998) 008.
[32] J. Gasser and H. Leutwyler, Phys. Rep. **87**, 77 (1982).
[33] E. Epelbaum, W. Glöckle, and U.-G. Meißner, Phys. Lett. **B439**, 1 (1998).
[34] V. G. Stoks, "The magnetic moment interaction in *NN* phase shift analysis," Ph.D. thesis, University Nijmegen, The Netherlands, 1990.
[35] E. Epelbaum, W. Glöckle, and U.-G. Meißner, Eur. Phys. J. A **19**, 125 (2004).
[36] J. A. Niskanen, Phys. Rev. C **65**, 037001 (2002).

[37] S. A. Coon and J. A. Niskanen, Phys. Rev. C **53**, 1154 (1996).
[38] N. Kaiser, R. Brockmann, and W. Weise, Nucl. Phys. **A625**, 758 (1997).
[39] T. Becher and H. Leutwyler, Eur. Phys. J. C **9**, 643 (1999).
[40] T. Fuchs, J. Gegelia, G. Japaridze, and S. Scherer, Phys. Rev. D **68**, 056005 (2003).
[41] R. Higa, nucl-th/0411046.
[42] E. Epelbaum, AIP Conf. Proc. **768**, 174 (2005).
[43] J. L. Friar, G. L. Payne, and U. van Kolck, Phys. Rev. C **71**, 024003 (2005).
[44] S. N. Yang and W. Glöckle, Phys. Rev. C **33**, 1774 (1986).
[45] J. A. Eden and M. F. Gari, Phys. Rev. C **53**, 1510 (1996).
[46] U. van Kolck, Phys. Rev. C **49**, 2932 (1994).
[47] V. Bernard, N. Kaiser, and U.-G. Meißner, Nucl. Phys. **A615**, 483 (1997).
[48] M. C. M. Rentmeester, R. G. E. Timmermans, and J. J. de Swart, AIP Conf. Proc. **768**, 59 (2005).